Catalysis Science & Technology

ROYAL SOCIETY OF CHEMISTRY

REVIEW

View Article Online
View Journal | View Issue

Cite this: *Catal. Sci. Technol.*, 2023, **13**, 4895

Photocatalytic conversion of carbon dioxide, methane, and air for green fuels synthesis†

Amira Chebbi,[a] Alessandro Sinopoli,[b] Ahmed Abotaleb[b] and Yusuf Bicer *[a]

Green fuels are derived from renewable resources that can replace or reduce the use of fossil fuels, and they can help reduce carbon emissions and dependence on finite resources including oil and natural gas. This review reports the latest investigations and studies on methane and carbon dioxide photocatalysis as well as nitrogen fixation for the production of green fuels. Specifically, methanol, formic acid, and ammonia synthesis were thoroughly reviewed to understand the corresponding chemical processes, experimental setups, and production strategies involved. The photocatalytic production of fuels from carbon dioxide and methane is generally affected by low yield and low selectivity, representing the main challenges of these processes. Whereas, a key issue in nitrogen photofixation is the fast oxidation of ammonia to nitrate during simultaneous redox reactions. Indeed, significant yield values were reported for methanol from the partial oxidation of methane (4500 μmol g^{-1} h^{-1}, Pd/H–TiO_2), methanol from carbon dioxide photoreduction (2910 μmol g^{-1} h^{-1}, 3% Cu–C/TiO_2), formic acid from carbon dioxide photoreduction (3500 μmol g^{-1} h^{-1}, g-C_3N_4/(Cu/TiO_2)), and ammonia from nitrogen fixation (3.81 mM g^{-1} h^{-1}, $In(OH)_3$/CN). To address the existing challenges and enhance efficiency, various solutions were introduced. For instance, developing photocatalysts with high surface area, fast separation of charges, large charge lifetime, photocatalyst performance, reaction conditions, efficient light absorption, appropriate band gap, changing reactor design, and the use of electron donors to consume the photogenerated electrons were proposed and adopted as potential solutions. Overall, this review provides insights into the opportunities and challenges associated with photocatalytic green fuel production from methane, carbon dioxide, and nitrogen and suggests potential avenues for future research and development.

Received 15th May 2023,
Accepted 2nd July 2023

DOI: 10.1039/d3cy00675a

rsc.li/catalysis

1. Introduction

Greenhouse gases, including carbon dioxide (CO_2) and methane (CH_4), contribute to global warming and climate change. Human daily activities, such as burning fossil fuels and deforestation, have led to the release of high carbon dioxide levels into the atmosphere. These increasing levels result in more frequent and longer-lasting natural disasters, including droughts, heat waves, flooding, forest wildfires, and acid rain. Statistics indicate that the global land and ocean surface temperature increased by 0.85 °C from 1880 to 2012, and the average global sea level rose by 0.19 meter.[1] Despite the fact that the amount of CO_2 released from burning fossil fuels, which is 29 Gt, is relatively minor compared to the 750 Gt released during the natural carbon cycle, it still contributes to the rising temperature and sea level because some of the CO_2 cannot be absorbed by the land and ocean.[2] Approximately 40% of excess CO_2 is absorbed, and the rest remains in the atmosphere. CO_2 emissions are mainly released from vehicles, heavy industries, chemical plants, and burning fossil fuels.[3] As shown in Table 1, the industrial sector is the third largest emitting greenhouse gases in the US, with 24% greenhouse gas emissions. Table 2 illustrates that in 2020, all economic sectors collectively contributed 79% of CO_2 emissions and 11% of CH_4 emissions.

Fig. 1 presents the emissions in metric tons of carbon dioxide equivalent from various industrial sectors in the United States. The data reveals that the leading sources of CO_2 emissions are fossil fuel combustion and those associated with natural gas and petroleum systems, accounting for 51% and 19.5% of the total emissions, respectively. Several studies have focused on finding alternative ways to reduce or eliminate the emissions of CO_2, and one of the most promising approaches is the photocatalytic process. It involves using light (potentially solar light) to activate and generate charges on the surface of

[a] *Division of Sustainable Development, College of Science and Engineering, Hamad Bin Khalifa University, Qatar Foundation, Doha, Qatar.*
E-mail: ybicer@hbku.edu.qa
[b] *Qatar Environment and Energy Research Institute, Hamad Bin Khalifa University, Qatar Foundation, P.O. Box 34410, Doha, Qatar*

† Electronic supplementary information (ESI) available. See DOI: https://doi.org/10.1039/d3cy00675a

Table 1 The US economic sectors and their associated greenhouse gas emissions in 2020

Economic sectors	Total US greenhouse gas emissions by economic sector in 2020
Transportation	27%
Electricity generation	25%
Industry	24%
Agriculture	11%
Commercial	7%
Residential	6%

Data retrieved from ref. 4.

Table 2 The greenhouse gases and their corresponding emissions

Greenhouse gases	US greenhouse gas emissions in 2020
Carbon dioxide (CO_2)	79%
Methane (CH_4)	11%
Nitrous oxide (N_2O)	7%
Fluorinated gases	3%

Data retrieved from ref. 4.

a semiconductor to perform oxidation or reduction reactions at mild conditions. This technology can be used to produce valuable chemicals, such as green fuels (low-carbon fuels), methanol (CH_3OH), formic acid (HCOOH), and ammonia (NH_3).

The aforementioned green fuels are highly advantageous due to their ease of handling, storage, and transportation, making them excellent energy carriers. NH_3, in particular, is widely used as a fertilizer and a significant source of hydrogen (H_2) due to its high H_2 density. CH_3OH serves as an alternative fuel, while HCOOH is used as a medium for storing H_2 and syngas. CH_3OH and HCOOH production offer a means of transforming excess CO_2 into valuable fuels, thus reducing CO_2 emissions.

The photocatalysis process induces chemical reactions by exposing a semiconductor photocatalyst to visible or UV light. Photocatalytic reactions comprise three steps: light absorption, charge separation, and product formation. During light absorption, photons are absorbed, and the subsequent charge separation results in the excitation of electrons from the valence band to the conduction band, creating positively charged holes. In the final step, product formation occurs through a redox reaction.[5] Among all photocatalysts, TiO_2 is considered a highly attractive option due to its strong reducing and oxidizing properties, low toxicity, and photostability.[3] However, its large band gap (3.2 eV) limits its ability to absorb visible light. Thus, modifications through doping with metals and metal-oxides are required. Over the last two decades, CO_2 obtained from carbon capture from other industrial processes, CH_4 and nitrogen gas, have been utilized as reactants in the photocatalytic production of valuable fuels, such as CH_3OH, NH_3, and HCOOH.

CH_4 represents the predominant constituent of natural gas, and has gained considerable traction as a fuel source due to its superior mass heat relative to other hydrocarbons. CH_4 is also a potent greenhouse gas, with a global warming potential (GWP) that is about 28–36 times higher than CO_2 over a 100-year timeframe, making it a significant contributor to climate change. This means that although CH_4 is present in lower concentrations compared to CO_2, it has a much stronger warming effect per unit of mass.

Together with being naturally produced through various biological and geological processes, CH_4 is also released during the production, processing, and transportation of fossil fuels, including coal mining, oil drilling, and natural gas extraction. CH_4 emissions from human activities, such as energy

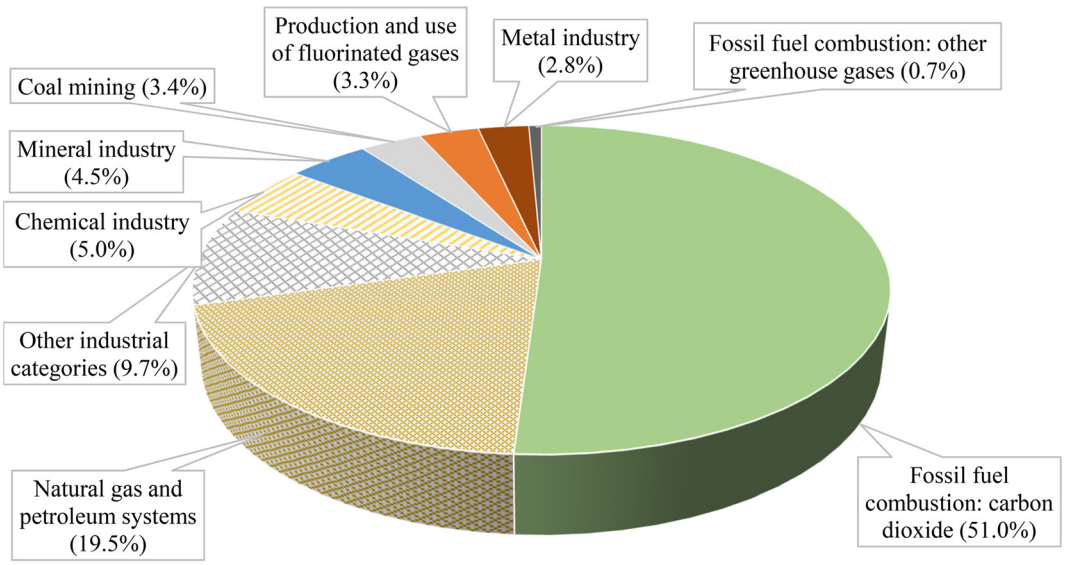

Fig. 1 Breakdown of the GHG emissions in million metric tons of carbon dioxide equivalent.[4]

production, agriculture, and waste management, contribute to the overall CH_4 concentration in the atmosphere. One significant source of CH_4 emissions is CH_4 flaring, which is the controlled burning of CH_4 during the extraction and processing of natural gas, petroleum, and coal.

CH_4 emissions, including those from CH_4 flaring, have significant environmental impacts and contribute to climate change. Strategies to reduce CH_4 emissions include improving CH_4 capture and utilization technologies, promoting more efficient energy production and consumption practices, implementing better waste management practices, and advancing agricultural and livestock management techniques.

According to scientific measurements and estimates, the global abundance of CH_4 in the atmosphere has increased over the past few decades. In 2021, the global average atmospheric CH_4 concentration was estimated to be around 1875 parts per billion (ppb), more than two and a half times higher than pre-industrial levels.[6] The increase in CH_4 abundance is attributed to various sources, including fossil fuel production and use, livestock and agricultural practices, natural wetland emissions, biomass burning, and waste management. Some of the major human-driven sources of CH_4 emissions include livestock production, rice cultivation, coal mining, oil and gas production and distribution, and landfill waste decomposition.[7–9] Moreover, CH_4 serves as a vital feedstock in numerous industrial chemical processes.[10] Nevertheless, the conversion of CH_4 in these procedures necessitates extreme conditions such as (temperature and pressure) conditions to facilitate the cracking of the C–H bond, which may impede CH_4 transformation mechanisms, causing carbon to further oxidize into unwanted byproducts.[11]

The main reserves of CH_4 are found in a variety of geological formations around the world. Some of the largest and most significant CH_4 reserves are located in the following regions:[12,13] Russia has some of the world's largest natural gas reserves, which are mainly associated with large oil fields, and are concentrated in regions such as the Yama Peninsula, the Barents Sea, and the Russian Arctic. Several countries in the Middle East, including Iran, Qatar, and Saudi Arabia, are known to have significant CH_4 reserves, which are often associated with large oil fields. The United States and Canada are also major producers of natural gas, with significant CH_4 reserves located in various regions. China has significant CH_4 reserves located in various regions, including the Sichuan Basin, the Trim Basin, and the Ordos Basin, among others. Thus, there are ongoing global efforts to monitor and reduce CH_4 emissions, including regulations, policies, and technological innovations to mitigate CH_4 emissions from various sectors and activities.

CH_4 conversion processes can be classified as steam CH_4 reforming (SMR), dry reforming of CH_4 (DRM), pyrolysis, and partial oxidation of CH_4 (POM). The steam CH_4 reforming (SMR) process involves using a catalyst to react CH_4 gas with steam, forming carbon monoxide (CO), H_2, and CO_2 as by-products. This is currently the most commonly used method for commercial H_2 production.[14] As an energy carrier, H_2 is highly regarded as one of the most promising options due to its reputation as the cleanest fuel, as its combustion solely generates water.[15] Furthermore, the combustion of H_2 produces more energy per unit of mass compared to traditional fossil fuels.[16,17] SMR releases large amounts of greenhouse gas (GHG) emissions associated with its production, making it less sustainable. The reaction takes place between 700 and 800 °C, consuming a high amount of energy, and a water gas shift (WGS) and CO_2 removal stage are added to obtain pure H_2 product.

DRM is used for the conversion of greenhouse gases into valuable chemicals and fuels. Under high operating pressure and temperature with a catalyst, the process involves the reaction of CH_4 and carbon to produce synthesis gas (syngas), which can be utilized in the Fischer–Tropsch process.[18–21] Over the past few decades, there has been significant research into the DRM as a means of generating syngas.[22]

While DRM can potentially be a promising route for converting two greenhouse gases into valuable products,[22] several limitations need to be addressed for its successful implementation at an industrial scale, including high process temperatures, carbon deposition, catalyst stability, and environmental considerations. DRM typically requires high temperatures (700–1000 °C) to achieve reasonable conversion rates. This can result in higher energy consumption and operational costs, as well as increased equipment and material requirements. Furthermore, during DRM, carbon deposition can occur on the catalyst surface. This leads to catalyst deactivation and reduced activity, increasing maintenance costs and limiting the overall process efficiency. DRM also requires catalysts that are capable of withstanding high temperatures and harsh reaction conditions. Finally, while DRM has the potential to reduce CO_2 emissions by converting it into valuable products, the overall environmental impact and sustainability of the process, including the capture, transport, and utilization of CO_2, need to be carefully evaluated.[23–25]

The pyrolysis of CH_4 is being recognized as a potentially viable method in shifting towards a sustainable H_2 economy.[26] CH_4 pyrolysis involves thermally decomposing CH_4 at high temperatures with the absence of oxygen to obtain H_2 and carbon as separate products. The most significant benefit of this approach is the production of carbon-free H_2, with only solid carbon left as a residue. This attribute provides CH_4 pyrolysis with a unique advantage over conventional methods such as steam CH_4 reforming and coal gasification.[27]

Currently, the ocean removes approximately a quarter of the current CO_2 emissions from human-centric activities.[28] Higher CO_2 levels absorbed in the seawater will alter the chemical buffering capacity of seawater, which affects and reduces the fraction of CO_2 emission taken up by the ocean.[29] CO_2 capture and conversion is a growing field of research and innovation, with various technologies being developed and tested worldwide.[30] One example of CO_2 capture and conversion technology is direct air capture

(DAC), which uses specialized chemical processes to capture CO_2 directly from ambient air.[31,32] Another example is carbon mineralization, which involves converting CO_2 into stable mineral forms through chemical reactions with naturally occurring minerals.[33]

There are also efforts to develop novel catalysts and electrochemical methods for converting CO_2 into valuable products, such as fuels, chemicals, and building materials. These technologies can potentially contribute to reducing greenhouse gas emissions and developing a circular economy by turning CO_2 into a valuable resource.[34,35]

To utilize CO_2 in eco-friendly processes, it is necessary to capture it from various industrial processes. CO_2 capture technologies can be classified as pre-combustion, combustion, and post-combustion. As a result of the gasification process, the fuel undergoes pre-combustion, which leads to the production of syngas primarily composed of H_2 and carbon monoxide. The subsequent step involves the conversion of H_2 and CO into CO_2; after that, it undergoes a separation of gas. This is generally recognized as pre-combustion technology.[36]

The second technology is the process of capturing gases during combustion, commonly referred to as "oxygen combustion". This process involves burning fuel in an environment enriched with oxygen to achieve optimal results.[36]

The capture of gases during the ultimate stage of releasing the combustion products is called post-combustion technology. This method is particularly effective for capturing CO_2 from various sources that generate energy, including thermal power plants and waste-to-energy facilities. Following the emission of flue gases, a suitable technology is utilized to separate CO_2 from other gases in a distinct process.[36]

NH_3 is a crucial chemical in the production of fertilizers, and it has many other applications, such as in the manufacture of chemicals, pharmaceuticals, and refrigerants. NH_3 has the potential to become an H_2 storage medium in the near future, thus enabling the development of CO_2-free energy systems. NH_3 is advantageous for H_2 storage due to its high volumetric H_2 density, low storage pressure, and long-term stability during storage. Additionally, NH_3 is viewed as a safe option because of its high auto-ignition temperature, low gas density, and lower condensation pressure compared to air.[37] NH_3 is known for its low cost, making it the most economical fuel choice (compared to LPG & gasoline).[38] As of now, the global production of NH_3 stands at approximately 200 million metric tons per year.[39]

Several different conversion technologies can be utilized for the production of NH_3, including Haber–Bosch, electrochemical, photocatalytic, and thermochemical cycle processes. The Haber–Bosh process is the most commonly used method for producing NH_3, accounting for approximately 85% of NH_3 production worldwide.[40] The synthesis of NH_3 involves the reaction of nitrogen and H_2 gas. It is an exothermic reaction that occurs spontaneously at low temperatures. Although the reaction is thermodynamically favorable at room temperature, the rate of reaction is too slow to be practical on an industrial scale.[37] Therefore, the reaction is set to occur at relatively high pressure (10–30 MPa) and temperature (400–500 °C). The challenge associated with this technology is the low conversion rate, even at high pressures.

The electrochemical conversion process involves the direct N_2 reduction, held at temperatures between 100–500 °C, on a catalyst surface able to adsorb and activate N_2 molecules.[41] Electrochemical NH_3 production has been gaining attention due to its potential benefits, such as higher energy efficiency compared to the conventional Haber–Bosch process. This process also offers environmental compatibility by utilizing carbon-free renewable energy resources, such as solar, tidal, and wind power. Another advantage is the elimination of fossil fuels as a source of H_2. Instead, the required protons (H^+) can be generated *in situ* through water oxidation.[41]

The thermochemical cycle process involves a sequence of chemical reactions in the absence of a catalyst at high temperatures of 1500 °C.[37] The process comprises two interconnected cycles: the reduction cycle for nitrogen activation and the steam-hydrolysis cycle for the formation of ammonia. The initial reaction is an endothermic process at high temperatures, which remains the main challenge associated with this technology, where aluminum nitride is produced by reducing alumina using carbon in an N_2 atmosphere. The subsequent reaction involves the hydrolysis of aluminum nitride to form NH_3 and alumina, which is then recycled back into the process.[42]

1.1. Methodology

A comprehensive search strategy was developed to identify relevant studies or articles for this review by searching for relevant literature in electronic databases, such as Elsevier, Scopus, ACS, Wiley, and Google scholar. Several publications on the photocatalytic conversion topic for the three fuels (CH_3OH, HCOOH and NH_3) were obtained. In this work, we mainly focused on the research and review papers published over the last 5 years.

1.2. Significance and contribution

This review aims to provide a comprehensive analysis of the current state of research on the photocatalytic conversion systems for green fuels. The significance of this review lies in its ability to synthesize and evaluate the vast and growing body of research on photocatalytic fuel production. By critically evaluating and summarizing research from multiple sources, this review paper includes the conversion systems for CH_3OH using two different pathways: photocatalytic reduction of CO_2 and photocatalytic partial oxidation of CH_4 (Fig. 2). Additionally, it evaluates the photocatalytic production of HCOOH and ammonia. This paper discusses the fuel synthesis method, challenges and potential solutions, and experimental setup, identifies knowledge gaps, highlights inconsistencies, and suggests potential avenues for future research. Overall, this review paper contributes to the advancement of scientific knowledge in photocatalytic processes that has the potential to make a meaningful contribution to the development of sustainable energy sources and the reduction of environmental impact.

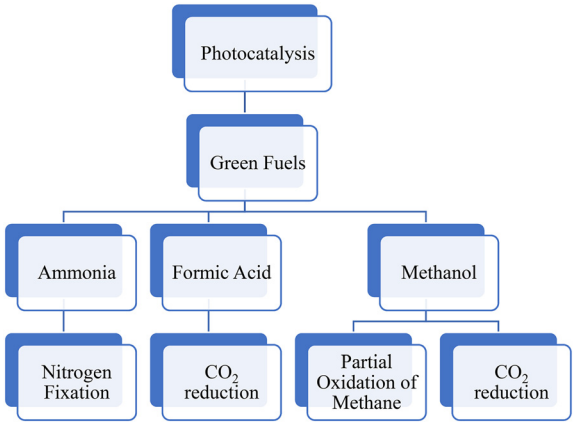

Fig. 2 The scope of the review.

2. Green fuels

Green fuels, also known as renewable fuels, biofuels, green hydrocarbons, and low carbon fuels, come from energy sources that are renewable and have a lower environmental impact compared to conventional fossil fuels, such as coal, oil, and natural gas.[43] Sharing similar chemical–physical properties to fossil fuels makes them fully infrastructure-compatible fuels. These fuels are derived from sustainable sources, including wind, solar, hydro, geothermal, and biomass, which enhance their eco-friendliness and reduce the greenhouse gas emissions associated with them.[44] CH_3OH, NH_3, and HCOOH are typical examples of green fuels.

GWP is a measurement that gauges the relative impact of various greenhouse gases on global warming. It quantifies the ability of a specific greenhouse gas to trap heat in the Earth's atmosphere over a defined period, typically 100 years, relative to carbon dioxide. We calculated the potential greenhouse gases produced during the complete combustion of the three fuels considered in this review: HCOOH, CH_3OH, and NH_3. This calculation included the presence of the GWP of water vapor, as it is considered the most abundant greenhouse gas in the Earth's atmosphere.[45] Total GWP of the reaction was calculated by multiplying the GWP of each greenhouse gas, produced by the complete combustion of the individual fuels, by the number of moles produced, and calculating the sum of products for each reaction. The GWP reported for CO_2 in the literature is 1,[46] and the GWP of water vapor was extracted from a study conducted by Sherwood *et al.*[45] and was found to be 5×10^{-4}.

The equations used to calculate the GWP of complete combustion products can be summarized as follows (eqn (1)–(3)):

$$\text{GWP of } CH_3OH = (1 \text{ mole} \times \text{GWP of } CO_2) + (2 \text{ moles} \times \text{GWP of } H_2O_{(g)}) \quad (1)$$

$$\text{GWP of HCOOH} = (2 \text{ moles} \times \text{GWP of } CO_2) + (2 \text{ moles} \times \text{GWP of } H_2O_{(g)}) \quad (2)$$

$$\text{GWP of } NH_3 = (1 \text{ moles} \times \text{GWP of } H_2O_{(g)}) \quad (3)$$

The calculated GWP values for CH_3OH, HCOOH and NH_3 combustion are 1.001, 2.001, and 0.0005 CO_2 eq., respectively. Here, complete NH_3 combustion stands out as an exceptionally clean process, yielding solely water vapor as GHG emissions, noting that there might be NOx emissions in the case of incomplete combustion. In contrast, the combustion of HCOOH fuel accounted for the highest impact of GHG on global warming. Consequently, NH_3 is widely acknowledged as the cleanest fuel option when subjected to combustion characteristics.

The growing awareness of the need to reduce the carbon footprint and mitigate climate change has led to a significant surge in the use of green fuels in recent years. The adoption of green fuels can facilitate the creation of a cleaner and more sustainable future. The following sections introduce the most recent technologies for green fuel production (CH_3OH, HCOOH, and NH_3) using photocatalytic processes.

2.1. Methanol production

CH_3OH is a widely used chemical in several industrial applications and processes. It is a valuable alternative fuel to LPG, gasoline, and gas oil.[47] Its ease of handling, storage, and transportation makes it a more advantageous energy carrier compared to H_2. Additionally, CH_3OH has several chemical derivatives, as shown in (Fig. 3). This section will be centered on the methods of producing CH_3OH, with a primary focus on the photocatalytic reduction of CO_2 and photocatalytic partial oxidation of CH_4.

Photocatalytic reduction of CO_2 uses carbon dioxide as a carbon source and raw material in the synthesis of CH_3OH. From an environmental perspective, transforming CO_2 into

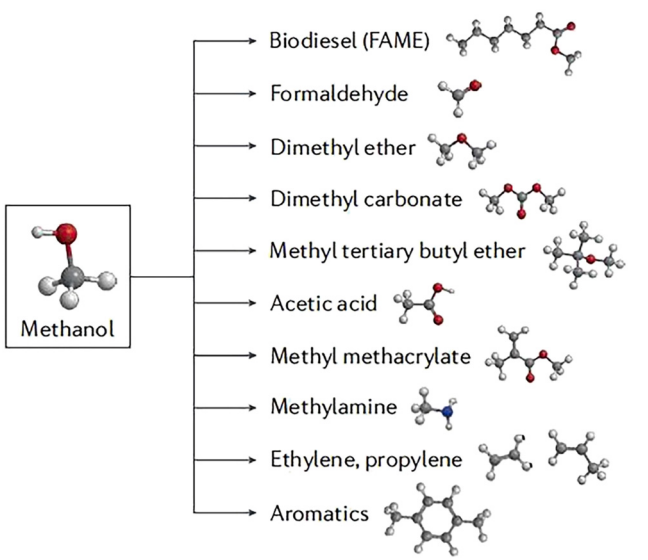

Fig. 3 Methanol chemical derivatives. Reproduced with permission from ref. 49.

other value-added products and fuels will help to reduce/limit global CO_2 emissions.

Photocatalytic partial oxidation of CH_4 is a process that uses CH_4 as a raw material, converting it to CH_3OH through a series of steps using light. CH_4 is one of the prospective substitutes for non-renewable petroleum resources since it can be converted to other added value-chemicals, such as syngas for NH_3 production and CH_3OH.[48] Currently, CH_3OH is produced using a thermal catalytic process in which syngas is produced (H_2 and CO) from steam reforming of CH_4 at high process conditions (very high temperature and pressure), and then hydrogenated to produce CH_3OH. Photocatalytic partial oxidation of CH_4 is an alternative way of producing CH_3OH at ambient temperatures and potentially using solar light; reducing the energy requirements means reducing the greenhouse gas emissions released to the atmosphere.

2.1.1 Photocatalytic reduction of CO_2 to methanol. The CO_2 photoreduction mechanism can lead to different products, primarily CO, CH_4, CH_3OH, and HCOOH, plus C_2 products, C_2H_2 and C_2H_5OH,[50] depending on the catalyst used in the photocatalytic reaction and reaction conditions, as reported in (Fig. 4). Several types of photocatalysts, such as metals, metal oxides, and metal–organic frameworks (MOFs), have been used.[51]

One of the earliest studies published on the photocatalytic reduction of CO_2 to CH_3OH was introduced by Solymosi and Tombácz.[53] Their work provided valuable insights into this emerging field, as they thoroughly investigated and explored the effect of catalysts and doping in photocatalytic CO_2 reduction products. 1% Rh/TiO_2/2% WO_3 exhibited a shift towards high CH_3OH selectivity compared to TiO_2 and TiO_2/0.1% WO_3, where no CH_3OH yield was observed.[53] Since then, extensive research has been conducted on the implementation of TiO_2 in photocatalytic CO_2 reduction under visible and UV irradiation, starting with the investigation of pristine TiO_2 and its subsequent combination with diverse materials to assess the impact of metal doping.[54–56]

A case study was conducted on a porphyrin-based MOF, where we observed a notable enhancement in the photocatalytic conversion of CO_2 to CH_3OH when Cu^{2+} was introduced. The presence of Cu^{2+} resulted in a remarkable sevenfold increase in the rate of CH_3OH production compared to the sample without Cu^{2+}.[57]

Other metal oxides, such as CeO_2/Bi_2MoO_6 nanocomposites, exhibit significant enhancements in specific surface area, visible light responsiveness, as well as improved efficiency in charge carrier separation and transfer compared to pure CeO_2 and pure Bi_2MoO_6.[58]

In 2018, Kavil *et al.*[3] conducted an experiment involving the production of CH_3OH from CO_2 using two samples of polluted seawater. The system used TiO_2 (P25), C/TiO_2, and $Cu–C/TiO_2$ doped catalysts under UV and visible light. Doping the photocatalyst with 3 wt% copper restricted the recombination of the electron–hole pair, and carbon modification reduced the TiO_2 band gap. Both modifications enhanced the photocatalytic reaction under UV and visible light. After 5 hours of UV light irradiation, the CH_3OH yields were 2910 mol g^{-1} and 2250 mol g^{-1}. However, 5 hours of natural sunlight irradiation resulted in CH_3OH yields of 990 mol g^{-1} and 910 mol g^{-1}. This difference has been attributed to the different concentrations of CH_4 in the samples. PSW-2 reported a quite high concentration of CH_4 (4.09 μM) compared to the PSW-1 (0.4 μM) system, and that is due to the presence of oxygen in the water samples. De-aeration caused a depletion of oxygen in PSW-1, producing methanogenic bacteria over CH_3OH production.[3] The production process requires six H_2 radicals to reduce CO_2 to CH_3OH (eqn (4)–(8)), and goes through the formation of formate radicals as reported below:

$$H_2CO_3 + e^- \rightarrow HCOO^{\bullet} + OH^- \quad (4)$$

$$HCO_3^- + H_2O + e^- \rightarrow HCOO^{\bullet} + 2OH^- \quad (5)$$

$$HCOO^{\bullet} + e^- \rightarrow HCOO^- \quad (6)$$

$$HCOO^- + H^+ \rightarrow HCOOH \quad (7)$$

The final step, the conversion of HCOOH to CH_3OH:

$$HCOOH + 3H_2O + 4e^- \rightarrow CH_3OH + 4OH^- \quad (8)$$

The experiment shown in (Fig. 5) was conducted using a stirred annular apparatus, including a glass reactor and CO_2 cylinder. The reactor was firmly connected to the CO_2 cylinder, and the polluted water samples were dosed at regular time intervals. The catalyst was added, and the glass reactor was purged with CO_2 for 60 minutes for saturation before light irradiation. The UV light was irradiated from all sides. Regarding the visible light experiment, the reactor was exposed to natural sunlight for 5 hours.

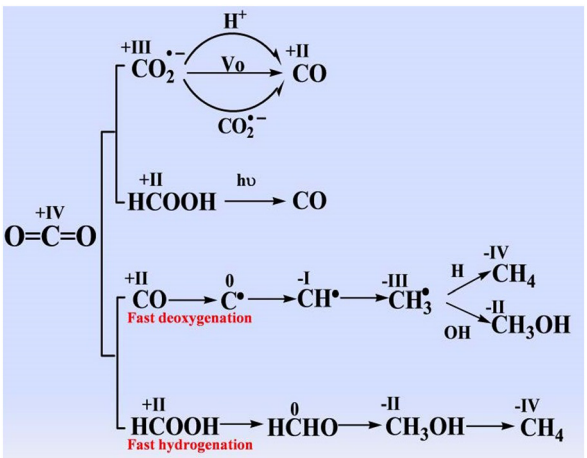

Fig. 4 Proposal of the reaction pathways for forming CO, CH_4, and CH_3OH in the photocatalytic CO_2 reduction. Reproduced with permission from ref. 52 under the terms of the CC BY 4.0 license.

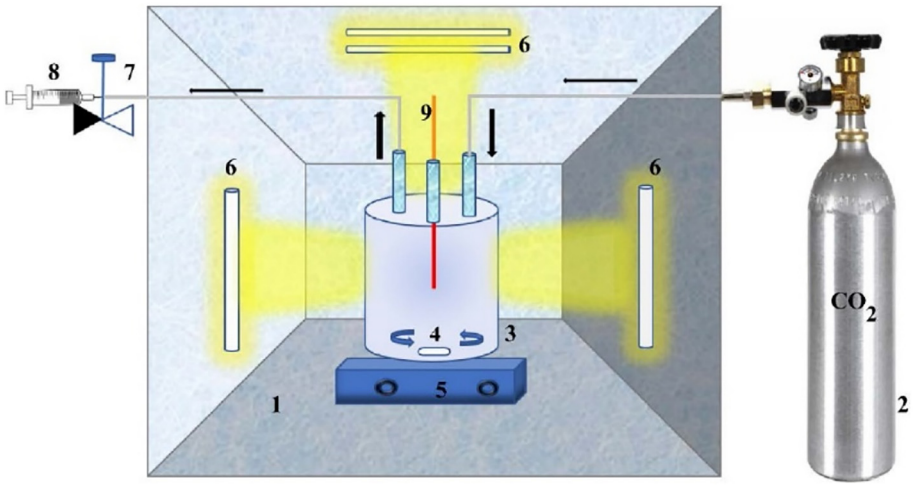

Fig. 5 Photocatalytic reduction diagram. Reproduced with permission from ref. 3 under the terms of the CC BY-NC-ND 4.0 license.

In the same year, Wang *et al.*[59] shed light on developing a photocatalyst capable of stably hydrogenating gaseous CO_2 to CH_3OH at ambient pressure with high selectivity. They reported a defect-laden indium oxide, $In_2O_{3-x}(OH)_y$, with a rod-like nanocrystal superstructure. Under simulated solar irradiation, this catalyst demonstrates a remarkable ability to hydrogenate CO_2 into CH_3OH with an impressive selectivity of 50%, which is much higher than for the other photocatalysts at that time.

Cobalt oxide (Co_3O_4) has also been employed for the photocatalytic production of CH_3OH using aqueous carbon dioxide (CO_2 aq) under solar light of 100 mW cm^{-2} without any sacrificial agent.[60] The aim of this experiment was to analyze the catalytic activity under ambient conditions of temperatures, pressures, and the quantity of CO_2 determined by the solubility of the gas in water at atmospheric pressure. Initially, the deionized water was saturated with CO_2 for one hour, followed by adding the photocatalyst to the CO_2 solution in a sealed reactor under stirring. The irradiation was conducted with a xenon lamp at ambient/room temperature for 6 hours. CH_3OH was detected in the gas phase but not in the liquid phase, which is attributed to the fact that the solution temperature reached 35 °C and caused the CH_3OH to evaporate. CH_3OH was the only product detected at the end of the experiment. Two reaction pathways are associated with this experiment, shown in Fig. 6. When CO_2 dissolves in water, it forms two products: CO_2 (aq) and carbonic acid (H_2CO_3). As a result, CO_2 and H_2CO_3, when reacting with protons (H^+), form CH_3OH as a final product. From different perspectives, both pathways have distinct advantages. In terms of concentration, the CO_2 (aq) pathway is favored because the concentration of CO_2 (aq) in solution is 500 times greater than that of H_2CO_3 in solution. However, the carbonic acid pathway is preferred regarding the reduction potential because H_2CO_3 has a more positive reduction potential.

Doping titania with metal nanoparticles represents a typical strategy to improve the performances of a photocatalyst. Shtyka *et al.*[61] reported on an investigation of gas phase CO_2 reduction using a series of TiO_2 loaded with various metals (Pt, Pd, Ni, and Cu) under continuous flow mode.[61] The study stated that Pt and Ni (2%) emerged as the most active catalysts among all of the investigated options, exhibiting a higher CH_3OH formation rate.

In the context of nanotechnologies, Kazemi Movahed *et al.*[62] performed a detailed study to thoroughly examine the preparation of copper oxide(I) nanoparticles on the nitrogen-doped carbon (N–C) rod-shaped core-shell nanostructure and its selective CO_2 reduction. CH_3OH was detected as the primary product.[62] The photocatalytic activity of Fe_3O_4@N–C/Cu_2O in CO_2 reduction was approximately four times greater than that of the Fe_3O_4@Cu_2O photocatalyst. This could be attributed to the improved absorption of visible light and the more efficient separation of photogenerated electron–hole pairs.

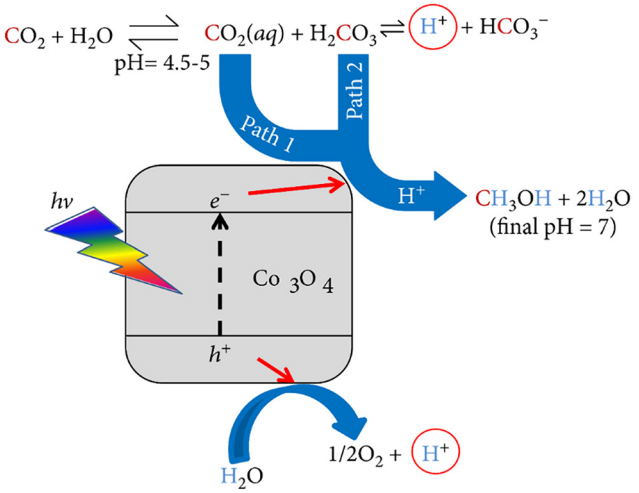

Fig. 6 Mechanism for the photocatalytic reduction of aqueous CO_2 in the presence of CO_3O_4. Reproduced with permission from ref. 60 under the terms of the CC BY 4.0 license.

In 2021, Albo & García[63] evaluated the performance of Mo_2C/TiO_2 heterojunctions in the continuous photocatalytic reduction of CO_2 to CH_3OH within a micro-optofluidic reactor, using both UV and visible LED lights (5 mW cm^{-2}) for illumination. The doping effect of Mo_2C on TiO_2 renders the composite material capable of exhibiting activity within the visible region compared to bare TiO_2, and additionally, it affects the morphology of TiO_2. When exposed to visible irradiation, these heterostructures demonstrate enhanced stability and recyclability in photocatalytic reactions. The experiment's results can be primarily attributed to the decreased bandgap energy, effective separation of electron–hole pairs, and enhanced interfacial conductivity.[63]

An interesting example focused on a copper-based photocatalyst is discussed by Xi *et al.*[64] Here, copper species with different valences are loaded onto TiO_2 through treatment in oxidizing and reducing atmospheres. These loaded species are referred as Cu/Ti(air) and Cu/Ti(H_2). Towards CO_2 photoreduction, Cu/Ti(H_2) demonstrated superior CH_3OH yield and selectivity compared to Cu/Ti(air), and that is due to the generation of oxygen vacancies through the reducing atmosphere, resulting in the availability of surface-adsorbed hydroxyl protons and photo-electrons on Cu/Ti(H_2).[64]

The photocatalytic reduction of CO_2 to CH_3OH using bismuth-promoted $BaTiO_3$ was the focus of a recent study conducted by Dasireddy & Likozar.[56] The doping of Ba/Bi to titania increased the TiO_2 band gap and enhanced the photocatalytic activity, producing a yield of 5.95 μmol g_{cat}^{-1} h^{-1}. The experiment demonstrated a high yield compared to other catalytic systems in the literature. Adding a metal ion acts as a photoelectron trap that reduces the recombination of electron–hole pairs. The experiment involved UV irradiation; the reactor was flushed with He to remove gas impurities such as trapped air. The main products associated with the experiment were carbon monoxide, H_2, and CH_3OH, plus trace amounts of other hydrocarbons.[56]

Not only metal oxide but also metal organic frameworks (MOFs) have been explored and analyzed in capturing CO_2 and its conversion into fuels with improved energy efficiency.[65] A metal–organic framework (MOF) is a crystalline material that consists of organic ligands coordinated with metal ions or clusters. MOFs possess a porous structure with high surface area, enabling them to adsorb efficiently and store gases or molecules. The study by Sonowal *et al.*[66] introduces the graphitic carbon nitride quantum dots-coupled Zr(IV)-based MOF composite (g-CNQDs@MOF) under visible light. The MOF composite (co-catalyst) exhibits excellent photochemical properties, which enhances the electronic conductance. As a result, the electron–hole separation was improved by extending the lifespan of photogenerated charge carriers on the surface of the composites. The presence of the excess electrons facilitated the rapid generation of catalytically active sites, resulting in the selective conversion of CO_2. The yield of CH_3OH was found to be 386 μmol $gcat^{-1}$ h^{-1} under visible light.[66] Significant advancements in this field (MOF-based composites) have resulted in a substantial increase in the CH_3OH yield. N. Li *et al.*[67] reported a method that involves encapsulating CuO quantum dots (QDs) within the pores of the metal–organic framework MIL-125(Ti) using a simple complexation–oxidation process. This composite photocatalyst is then formed by combination with g-C_3N_4, resulting in g-C_3N_4/CuO@MIL-125(Ti) with a CH_3OH yield of 997.2 μmol g^{-1}.[67]

Recently, a study was conducted by H. Yu *et al.*[68] where a novel multicomponent hetero-structure photocatalyst has been developed. It demonstrates the efficient and stable photoreduction of CO_2 in water, producing CH_3OH as the primary product, using a triphase reaction system (gas–liquid–solid interfacial system). The catalyst developed was $SrTiO_3$ (LaCr)/Cu@Ni/SiO_2/TiN. Observations point to the fact that the photocatalyst demonstrates exceptional light absorption capabilities and effectively separates charge carriers. In fact, the triphase interfacial system enhances the efficiency of photocatalytic CO_2 to CH_3OH conversion by an impressive 50-fold compared to the diphase interfacial system. This study successfully achieves the low-cost and highly efficient photocatalytic CO_2 reduction to CH_3OH.[68] Table 3 provides a concise summary of the catalysts that have been investigated and reported concerning photocatalytic reduction.

2.1.2 Photocatalytic partial oxidation of methane to methanol (POM). One of the early explorations in the field of CH_4 photoconversion to CH_3OH was conducted by Ogura & Kataoka in 1988.[71] The reaction introduced was water vapor and CH_4 at standard atmospheric pressure. The typical POM mechanism is shown in (eqn (9)–(12)) and Fig. 9. When water gets exposed to photons, it produces hydroxide radicals ($^{\bullet}OH$) (eqn (10)). The hydroxyl radical further reacts with CH_4 to form a methyl radical ($^{\bullet}CH_3$) (eqn 11). The final step is the reaction of the methyl radical with water to form CH_3OH (eqn 12). One promising catalyst for the photo-partial oxidation of CH_4 is TiO_2, which has been extensively studied due to its high stability and photocatalytic activity.[72,73] Other catalysts, such as WO_3, Bi_2WO_6, and ZnO, have also been investigated. The photocatalytic performance of these materials can be improved by doping with metal ions or modifying the surface.[74–76] A few review papers have been recently published on photo-partial oxidation of CH_4, and we invite the reader to consult them for a deeper knowledge of the topic.[48,77,78]

$$H_2O + h\nu \rightarrow h_2 + \frac{1}{2}O_2 \quad (9)$$

$$H_2O + h\nu \rightarrow \frac{1}{2}H_2 + {}^{\bullet}OH \quad (10)$$

$$CH_4 + {}^{\bullet}OH \rightarrow {}^{\bullet}CH_3 + H_2O \quad (11)$$

$$CH_3 + H_2O \rightarrow CH_3OH + \frac{1}{2}H_2 \quad (12)$$

In 2008, Y. Hu *et al.*[79] prepared catalysts containing V in MCM-41 (vanadium in MCM-41 mesoporous material) using

Table 3 Performance of CO_2 reduction and its corresponding methanol yield

Catalyst	Main products	CH_3OH yield (μmol $gcat^{-1}$ h^{-1})	Light irradiation	Ref.
P25	CO	0.045	Visible	54
20% $FeTiO_3/TiO_2$	CO, CH_3OH, or CH_3	0.43	Visible	54
g-C_3N_4/ZnO	CH_3OH	0.6	Visible	69
$In_2O_{3-x}(OH)_y$	—	60	—	70
3% Cu–C/TiO_2	CH_3OH	2910	UV	3
CeO_2/Bi_2MoO_6 (5C-BM)	CH_3OH and C_2H_5OH	32.5	Visible	58
CeO_2	CH_3OH and C_2H_5OH	5.1	Visible	58
Bi_2MoO_6	CH_3OH and C_2H_5OH	17.6	Visible	58
Fe_3O_4@N–C/Cu_2O	—	146.7	Visible	62
Cu_2O/TiO_2	CH_3OH	9–13	UV	55
Cu_2O/TiO_2	CH_3OH	12–70	Visible	55
Mo_2C/TiO_2	—	11.8	UV-vis	63
Cu/Ti(H_2)	—	—	Visible	64
(g-CNQDs@MOF)	—	386	Visible	66
BiO/TiO_2	CO, CH_4, H_2	0.52	UV	56
BaO/TiO_2	CO, CH_4, H_2	0.65	UV	56
$BiTiO_3$	CO, CH_4, H_2, CH_3OH	3.83	UV	56
$BaTiO_3$	CO, CH_4, H_2, CH_3OH	4.37	UV	56
$BiO/BaTiO_3$	CO, H_2, CH_3OH and CH_4	5.95	UV	56
Cu_xO/TiO_2	CO, CH_4 and CH_3OH	53.75	Full spectrum	64
$SrTiO_3$ (LaCr)/Cu@Ni/SiO_2/TiN	CH_3OH, C_2H_5OH, CH_4, and CO	25.8	Visible	68

a direct synthesis technique in both acidic and basic conditions, and through impregnation. The catalysts were subjected to UV irradiation at 295 K for the selective oxidation of methane with nitric oxide (NO) to evaluate their photocatalytic performance. Notably, the V-MCM-41 catalyst prepared in an acidic solution and impregnated V/MCM-41 exhibited the formation of CH_3OH with high selectivity.[79]

The group of Murcia-López *et al.*[80] successfully synthesized and characterized photocatalysts based on bismuth for the first time, including Bi_2WO_6, $BiVO_4$, and a coupled Bi_2WO_6/TiO_2-P25. The photocatalysts were investigated with UV-visible radiation for their ability to selectively oxidize methane to CH_3OH. Among the photocatalysts obtained, $BiVO_4$ stands out as the most promising catalyst for this specific reaction, exhibiting superior selectivity towards CH_3OH production and greater stability compared to the other catalysts.[80]

The Bi_2O_3 photocatalyst was investigated by de Oliveira *et al.*,[81] for CH_4 reforming to CH_3OH under visible light at ambient temperature and pressure. The production rate of CH_3OH was approximately 3771 μmol g^{-1} h^{-1} and a selectivity of 65%. The photooxidation was conducted in a 150 mL homemade-quarts reactor (Fig. 7) at ambient conditions (25 °C and atmospheric pressure). A mass of 100 mg Bi_2O_3 was

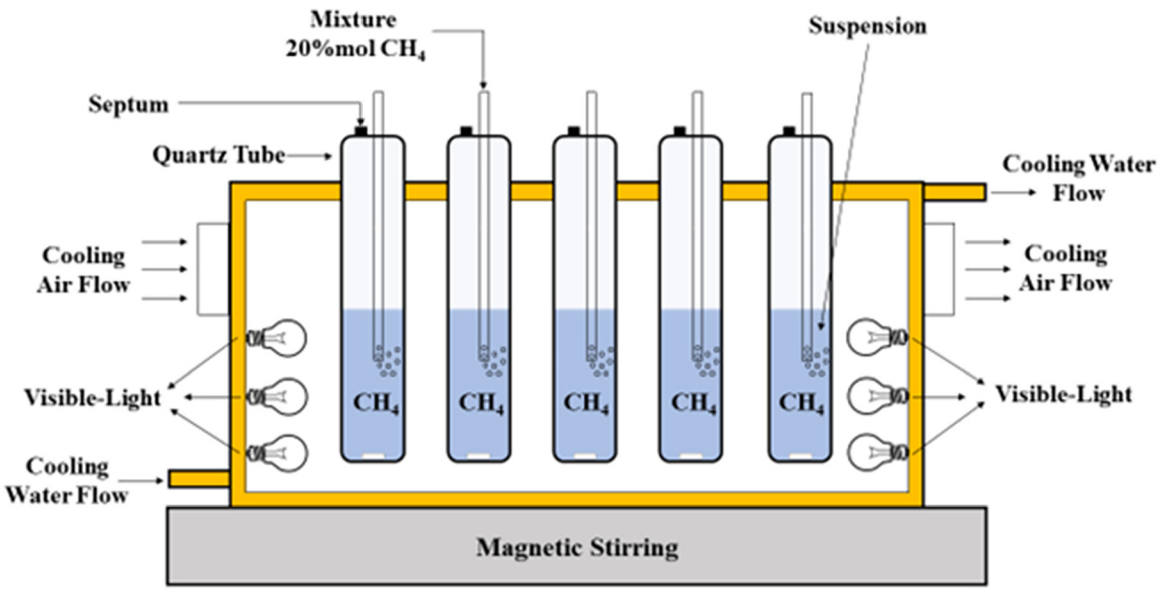

Fig. 7 Experimental setup for the photocatalytic partial oxidation of CH_4 to CH_3OH. Reproduced with permission from ref. 81.

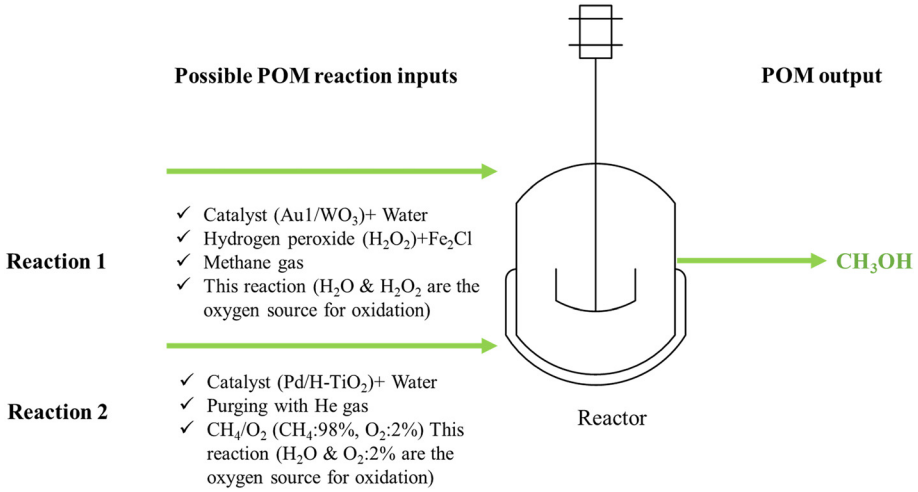

Fig. 8 Possible POM inputs with different reaction conditions.

added to 100 mL deionized water, along with purging the suspension with a CH_4 mixture containing 20% mol CH_4 in argon. The flow was interrupted and sealed with Teflon-lined caps after 30 minutes. The reaction was operated for 4 hours under six 18 W lamps.[81]

As discussed in the previous section, doping metal oxide with metal nanoparticles is a common strategy in photocatalysis. In this regard, a study was conducted on the photocatalytic conversion of CH_4 to CH_3OH using tungsten trioxide with atomically dispersed gold.[82] The production rate of CH_3OH reached up to 589 μmol g^{-1} h^{-1}. The light source was a 300 W xenon lamp providing visible light ($\lambda \geq 420$ nm). 20 mg of catalyst was dispersed in 20 mL deionized water, then 200 μl H_2O_2 and Fe_2Cl (0.01 M, 2 mL) were added to the catalyst solution to obtain the precursor solution. The precursor solution was placed in the reactor. Thereafter, the reactor was purged by CH_4 to remove O_2 and air. Then, CH_4 was introduced at a pressure of 2 MPa, and the reaction was held at 25 °C for 1 hour. After cooling down the system, the products were evaluated using an ice bath for 1 h to recondense potential CH_3OH vapors.

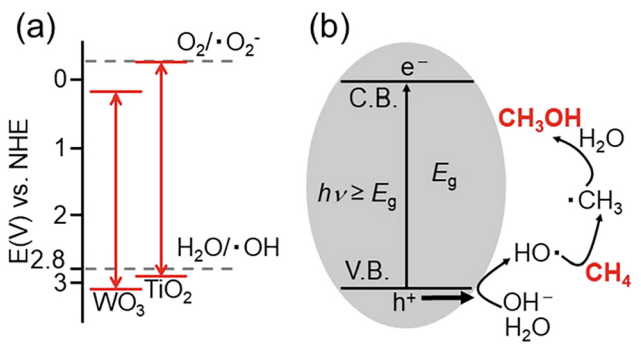

Fig. 9 Typical photocatalytic partial oxidation of methane to methanol mechanism catalyzed by metal oxide. (a) Redox potentials of WO_3 and TiO_2. (b) Mechanism of the conversion of CH_4 to CH_3OH by photocatalytic reaction. Adapted with permission from ref. 84 under the terms of the CC BY 3.0 license.

Similarly, X. Zhang *et al.*[83] developed a hollow porous Pd/H–TiO_2 photocatalyst to perform the successful photocatalytic oxidation of CH_4 using O_2 gas. The experiment was held under mild conditions and light irradiation. The resulting production rate of CH_3OH was found to be 4500 μmol g^{-1} h^{-1}, with a selectivity of up to 70%. To perform the experiment, 10 mg catalyst was dispersed with 60 mL H_2O and placed into a stainless-steel reactor with a quartz window. After purging He gas, CH_4/O_2 (CH_4: 98%, O_2: 2%) was introduced to the reactor, followed by light irradiation using a 300 W xenon lamp.[83]

To enhance efficiency and achieve successful CH_3OH production, modifications to the reaction conditions can be made, as indicated in Fig. 8.

Recently, J. Wang *et al.*[85] conducted a photocatalytic conversion of CH_4 to CH_3OH under mild conditions, using BiOCl with oxygen vacancies under visible light irradiation in NaCl aqueous solution with H_2O_2 to promote the oxidation. The CH_3OH production rate was 180.75 μmol g_{cat}^{-1} h^{-1} with 80.07% selectivity. Prior to the reaction, a mixture of CH_4 (10%) and nitrogen (90%) was continuously purged through the reactor for 30 minutes under dark conditions to eliminate any atmospheric air. Ultimately, the reactor was sealed and exposed to a 500 W xenon lamp for one hour.[85]

Another recent interesting study was reported by Du *et al.*[86] using AuFe–ZnO as a bifunctional catalyst. The study yielded 1365 μmol g^{-1} h^{-1} with high selectivity of CH_3OH up to 90.7%. The reaction was performed in a 100 mL autoclave reactor with a quartz window, with 40 mg of photocatalyst dispersed in 20 mL of water. The reactor was then pressurized with 2 bar O_2 and 18 bar CH_4 after being purge-gassed with oxygen (O_2) multiple times to remove air. The photocatalytic reaction was irradiated using a 300 W Xe lamp at 20 °C. After the reaction, the mixture was cooled to 10 °C.[86] Table 4 outlines a comprehensive collection of catalysts investigated and reported in the context of POM reactions.

2.1.3 Challenges and potential solutions. Herein, we list the main challenges and linked solutions for CO_2 reduction and partial oxidation of CH_4 to CH_3OH in Table 5.

Table 4 Performance of POM catalysts and its methanol yield and selectivity

Catalyst	Temperature	Product	Yield μmol g^{-1} h^{-1}	Selectivity	Ref.
WO_3/F	55 °C	CH_3OH, C_2H_6, CO_2	—	17.90%	75
WO_3/H_2O_2	55 °C	CH_3OH, C_2H_6, CO_2	—	13.70%	75
WO_3/Fe^{3+}	55 °C	CH_3OH, C_2H_6, CO_2	67.5	58.50%	76
WO_3	55 °C	CH_3OH, C_2H_6, CO_2	27.1	46%	76
0.12 wt% Au/TiO_2	25 °C	CH_3OH	150	30%	72
FeOOH/m-WO_3	25 °C	CH_3OH, C_2H_6, and CO_2	211.2	91%	74
Co–$SrTiO_3$	80 °C	—	1840	98.7%	73
Bi_2O_3	25 °C	CH_3CH_2OH, CH_3CO_2H, $(CH_3)_2CO$, CH_3OH	3771	65%	81
Au1/WO_3	25 °C	CH_3OH, HCHO	589	75%	82
BiOCl	25 °C	CH_3OH, HCOOH	180.75	80.07%	85
Pd/H–TiO_2	45 °C	CO_2, HCHO, CH_3OH	4500	70%	83
AuFe–ZnO	20 °C	CH_3OOH, HCHO, HCOOH, CO, and CO_2	1365	90.7%	86

2.1.4 Research gaps. The following research gaps shown in Fig. 10 are identified based on the previous literature work.[47,87,88]

Catalyst development is a critical area requiring further research and development. Although several catalysts have been reported, they often suffer from low selectivity, stability, or activity. Additional research is required to design catalysts with properties such as high efficiency, enduring stability, fast kinetics, high selectivity, and low manufacturing cost. Moreover, understanding the mechanism of the reaction is crucial, and the specific reaction pathways lack clear understanding. Further research and evaluation are needed to identify the intermediates involved in the reaction, their stability, and their role in the overall reaction. For example, carbon-based materials are unique and can function as light absorbers, catalysts, or both, owing to their electronic properties and intrinsic high charge transport. Additional work is required to fully understand the advantages of carbon-based support and viability (cost).

The effect of light on the reaction mechanism is not adequately perceived. A deeper exploration is mandatory to understand the effect of different wavelengths of light on the reaction rate and selectivity. In terms of energy efficiency, although the process has the potential to use renewable energy sources such as solar energy, the overall energy efficiency of the process is often low. Extended research efforts are necessary to develop systems that efficiently produce CH_3OH using renewable energy sources. For this reason, future studies should focus more on the life cycle assessment. A comprehensive life cycle of CO_2 photoreduction and POM technologies is required. This includes assessing the environmental impact of the entire process, from the extraction of raw materials to the disposal of waste products. Such an assessment will help identify the potential environmental benefits and limitations.

Scaling up is another area of concern for photocatalytic technologies. When seeking sustainable and renewable methods alternative to conventional processes, the following should be considered: stability, durability, and economic viability related to the reaction and the process in general. Extended research efforts are necessary to address these knowledge gaps. An attractive approach could be integrating photocatalytic CO_2 conversion with other processes, such as CO_2 capture and storage, to create a complete carbon capture and utilization system.

2.2. Photocatalytic reduction of CO_2 to formic acid.

HCOOH is a commonly used chemical raw material characterized by relatively non-toxic and non-corrosive properties.[89] As a result, it is considered a source of H_2 or CO that is safe, easy to handle, and transport for a variety of reactions, especially in fuel generation.[89,90] Furthermore, it can be used as important

Table 5 The challenges associated with CO_2 reduction and partial oxidation of methane to methanol and possible solutions

Challenges	Solutions
• Insufficient catalytic stability	✓ Use and modify catalysts with high surface area and high porosity
• Fast recombination of electron–hole pair, large band gap	✓ Doping the catalysts with metals, metal oxides, and non-metals or using metal–organic framework (MOFs) catalysts
• Lack of selectivity	✓ The use of innovative reactors and optimizing reaction conditions (temperature, pressure, and light intensity)
• In case of using polluted seawater, oxygen depletion causes the production of methanogenic bacteria over CH_3OH production	✓ Introducing additional oxygen sources
• Low CH_3OH yield	✓ Use the suitable catalyst dosage while improving the light absorption properties of the material
• Very high catalyst concentration can reduce CH_3OH yield due to the turbidity of suspension, which stops the light source from penetrating, whereas surface agglomeration diminishes the active sites available for the reaction	✓ Observe the effect of increasing catalyst dosage on the CH_3OH yield until you examine a decrease in the CH_3OH yield

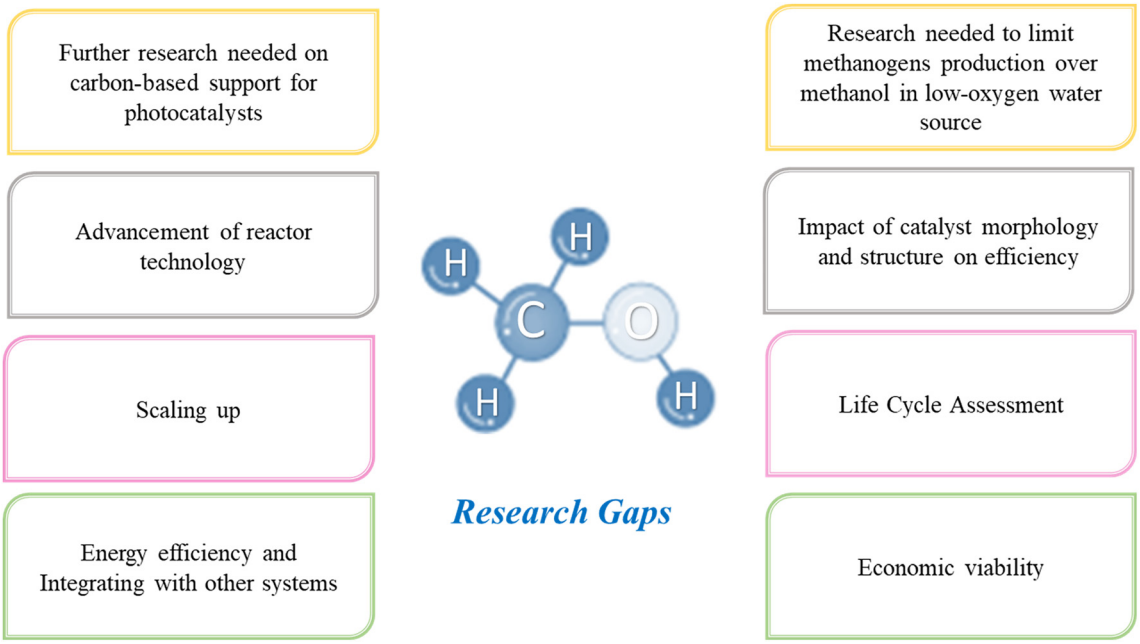

Fig. 10 Knowledge gaps related to the photocatalytic production of methanol.

feedstock to produce CH_3OH and other fine chemicals, plus it can substitute other inorganic acids as it is considered as the less corrosive among them.

HCOOH is one of the valuable derivatives of CO_2 reduction.[89] It can be produced through a photocatalytic reaction of CO_2 in the presence of water and a photocatalyst (semiconductors doped with other substances), as shown in Fig. 5. Various products can be generated through CO_2 photoconversion, which can occur *via* distinct mechanisms, as illustrated in Fig. 11. In general, HCOOH and CO are the most generated products from the CO_2 reduction process.[91]

Back in 1989, an important study by Aliwi and Al-Jubori[93] was revealed to the scientific community as it revealed one of the earliest investigations into the world of photocatalytic CO_2 reduction to HCOOH. The photoreduction uses metal sulfide semiconductors (n-Bi_2S_3 and n-CdS) in the presence of H_2S. The presence of hydrogen sulfide was found to increase the rate of the photoreduction processes. This study holds significant interest; however, to what extent can H_2S be safely used and handled due to its toxic properties, even at relatively low concentrations? This is why the attention has been focused on developing more safe and sustainable oxide-based photocatalysts (Table 6).

A study by Maeda *et al.*[94] successfully showcased the capability of a polymeric carbon nitride semiconductor in the photocatalytic conversion of CO_2 into HCOOH under visible light. This process exhibits exceptional performance metrics, including a selectivity of >80% achieved by combining the semiconductor with a molecular ruthenium complex acting as a catalyst.[94]

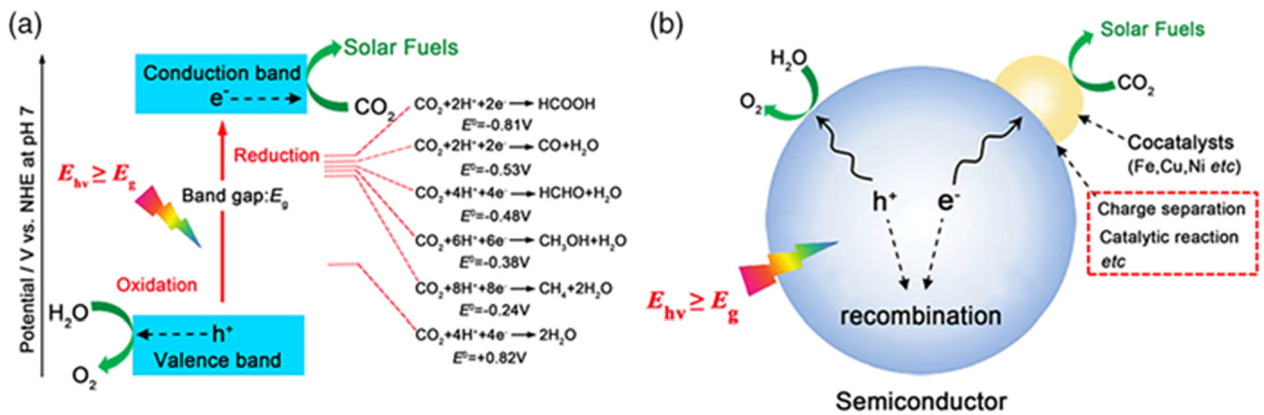

Fig. 11 Schematic diagram of the photocatalytic reduction of CO_2 to solar fuels. (a) Energy diagram for CO_2 reduction and water oxidation on a semiconductor. (b) Schematic of the photocatalytic reaction process and influencing factors. Reproduced with permission from ref. 92 under the terms of the CC BY-NC-ND 4.0 license.

Table 6 Performance of catalysts for CO_2 reduction to formic acid

Catalyst	Temperature	Product	Yield (HCOOH)	Ref.
TiO_2–CuPc	25 °C	HCOOH	208.5 μmol g^{-1} h^{-1}	102
PdAu@Fe_2Mn-MOF	25 °C	HCOOH	725 μmol g^{-1}	98
InPc	26 °C	Formate	—	96
H–TiO_2	—	HCOOH–CO	—	97
α-FeOOH/Al_2O	25 °C	HCOOH, CO and H_2	—	100
Ru–N_2CTF	—	Formate	2090 μmol g_{cat}^{-1} h^{-1} (formate)	101
N–TiO_2/CuO	50 °C	HCOOH, H_2	33 μmol g^{-1} min^{-1}	99
TiO_2/CuO	50 °C	HCOOH, H_2	26 μmol g^{-1} min^{-1}	99
N–TiO_2/CeO_2/CuO	50 °C	HCOOH, H_2	28 μmol g^{-1} min^{-1}	99
N–TiO_2/CeO_2	50 °C	HCOOH, H_2	2 μmol g^{-1} h^{-1}	99
TiO_2/CeO_2/CuO	50 °C	HCOOH, H_2	25 μmol g^{-1} min^{-1}	99
TiO_2	50 °C	HCOOH, H_2	0.9 μmol g^{-1} min^{-1}	99
g-C_3N_4/(Cu/TiO_2)	25 °C	HCOOH, CH_3OH	3500 μmol g^{-1} h^{-1}	103

A comprehensive study was conducted by Nakada *et al.*[95] to examine the photophysical, photochemical, and photocatalytic capabilities of a binuclear complex (RuReCl) containing a Ru(II) photosensitizer and a Re(I) catalyst unit connected by a bridging ligand in aqueous solution. Remarkably, RuReCl demonstrated its ability to catalyze the reduction of CO_2 using ascorbate as an electron donor. Notably, HCOOH was the main product generated from the photocatalytic reaction in the aqueous solution.[95]

In 2020, a study by Omadoko *et al.*[96] provided insights into the conversion of carbon dioxide into HCOOH under acidic conditions and formate under basic or neutral conditions. The method employed photoreduction, utilizing an affordable setup comprising titanium dioxide, metal phthalocyanines (PC), and an inexpensive incandescent source. It was found that InPC exhibits a more significant generation of formate when compared to NiPC, ZnPC, and CuPC, resulting in a higher quantity of formate production. This can be attributed to the lowest degree of aggregation of InPC promoting electron transfer reactions.

Instead, H. Zhang *et al.*[97] investigated HCOOH production using a different approach: the hydride transfer pathway for the photocatalytic reduction of CO_2 on TiO_2. In this experiment, using UV light, hydrogenated TiO_2 functions as a hydride donor for the selective reduction of CO_2. The experiment involved treating TiO_2 with both argon (Ar) and H_2. Ar-treated TiO_2 produced CO and hydrogen-treated generated HCOOH as a product. Electron paramagnetic resonance (EPR) and X-ray photoelectron spectroscopy (XPS) analyses illustrated that the O-vacancy was predominant on Ar-treated TiO_2, while the H_2-treated TiO_2 exhibited H on the surface. The findings prove that hydrogenation can generate hydride-like sites, allowing TiO_2 to function as a hydride reagent to directly participate in the CO_2 photocatalytic reduction process to HCOOH. The hydride transfer (H–) to CO_2 enhances the C–H bond formation and the HCOOH production. However, hydride transfer may not be restricted to CO_2 reduction; it can also be implemented in the H_2 evolution process in further studies.[97]

The advent of MOFs also played a role in the photoconversion of CO_2 to HCOOH. Mori *et al.*[98] documented the results of the photoreduction of CO_2 to formic acid by Fe-based MOFs. The study examined how heteroatom doping and the confinement of Pd alloy nanoparticles (NPs) influenced an amine-functionalized Fe-based metal organic framework (Fe_3-MOF). It was observed that the electron–hole separation efficiency of the photocatalysts was enhanced through the incorporation of Pd and Au NPs, which acted as electron scavengers for excited electrons. The research paper revealed that the HCOOH production of PdAu@Fe_2Mn-MOF was 3.6 times higher than that of the unmodified Fe_3-MOF.[98]

Mixed oxide composite catalysts have been investigated by Ibarra-Rodriguez *et al.*[99] In their work, the photocatalytic reduction of CO_2 to produce HCOOH and H_2 with visible light using activated N–TiO_2/CeO_2/CuO composites was assessed. Specifically, the ternary titania-based compounds were synthesized by implementing two steps, pure and nitrogen-doped titanium dioxide, followed by adding 3% wt of cerium and copper oxide particles. Due to the synergy effect of the urea precursor, the nitrogen-doped composite resulted in a higher surface area. A mixed valence state of Ti and the presence of oxygen vacancies was observed during the characterization, which is responsible for the higher adsorption of the desired molecules. N–TiO_2/CuO generated the highest HCOOH yield (33 μmol g^{-1} min^{-1}), as indicated in Fig. 12, with better CO_2 adsorption capacity and following a Z-scheme where the charges are efficiently separated. On the other hand, adding the CeO_2 co-catalyst reduced the HCOOH yield due to its affinity towards adsorbing CO_3^{-2} and OH ions that could occupy the active sites. However, N–TiO_2/CeO_2/CuO results in the maximum production of H_2 due to its highest Ti^{3+}/Ti^{4+} valence state ratio, resulting in more active sites for water adsorption, and therefore, the production of H_2. The experiment was conducted at room temperature; the composite powder was added to the water, followed by the addition of CO_2 gas to the solution for 15 minutes in a batch reactor. The system's pressure was 2 psi and irradiated for three hours using two xenon lamps.[99]

The findings of a study reported by An *et al.*[100] offer fresh insights into employing a recyclable solid catalyst with an appropriate support material that constitutes a different approach for catalyst activation in achieving selective CO_2

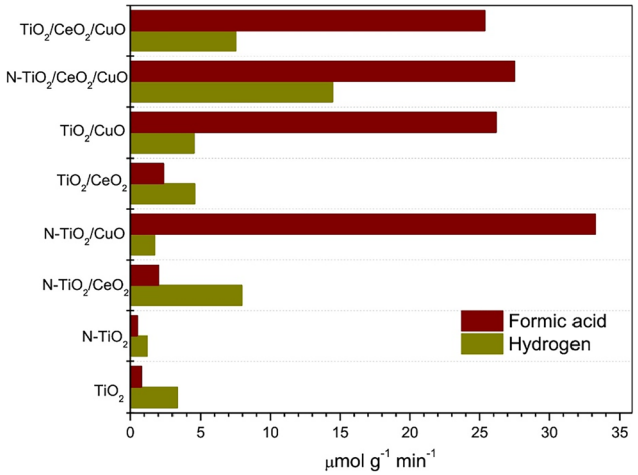

Fig. 12 Formic acid and hydrogen yields reported for different metal oxide composites. Reproduced with permission from ref. 99 under the terms of the CC BY-NC-ND 4.0 license.

reduction. This group presented a widely available soil mineral alpha-iron(III) oxyhydroxide (α-FeOOH; goethite) that was loaded onto an Al_2O_3 support, and tested under visible light. The reaction was conducted in the presence of a Ru^{II} photosensitizer and 1-benzyl-1,4-dihydronicotinamide (BNAH) as an electron donor.[100]

Recently, building upon prior research, Wang *et al.*[101] embarked on an experimental work that expanded our understanding of the negative impact of uncontrolled and non-uniformly dispersed active sites on the selectivity and activity. The authors introduced a novel *in situ* covalent-bonding approach to integrate the precisely defined single-site $Ru–N_2$ species into conjugated covalent triazine frameworks (CTFs) for achieving a remarkably selective photoreduction of CO_2. The resultant Ru-CTF structure was found to enhance the charge separation and provide stability to the molecular catalyst, thereby facilitating a solar-to-formate conversion.[101] Table 6 presents a concise compilation of the catalysts examined and reported in studies focusing on the photocatalytic CO_2 reduction to HCOOH.

2.2.1 Challenges and potential solutions. Within this section, Table 7 is presented, highlighting the primary challenges involved in the reduction of CO_2 to HCOOH.

2.2.2 Research gaps. The following research gaps are identified based on the previous literature work as shown in Fig. 13.

The effectiveness of direct HCOOH production using photons *versus* the generation of electrons through photovoltaics followed by electro-catalyst use for HCOOH depends on various factors, including efficiency, cost, and application requirements. Since both approaches are under development, several criteria should be investigated, such as the efficiency of the process, the ability of both processes to meet the industrial demand, and the technological maturity. Additionally, one of the most important factors is the environmental impact. Hence, evaluating factors such as the carbon footprint, energy consumption, and the potential environmental impacts, including the generation of pollutants or by-products, associated with each method can contribute to assessing the sustainability and desirability of the production approach.

Further development of the large-scale photoreduction of CO_2 and assessing the feasibility of the photoreactors require careful consideration of various factors, the availability of the light source, the cost, energy consumption, process control and automation (reaction conditions), and maintenance. Moreover, understanding the reaction kinetics and efficient mass transfer is vital as it directly influences the process efficiency and the resulting products.

2.3. Ammonia production through nitrogen photofixation

NH_3 is a widely used chemical fertilizer that has significantly raised agricultural output worldwide.[104] It is a significant energy carrier that can easily be condensed, stored, and transported. Due to its high H_2 density (17.6 wt%) and low liquefying pressure, NH_3 is also a promising H_2 source. It can potentially be a significant focal point in a future H_2 economy. H_2 can be easily extracted from NH_3 when needed. On the other hand, the current Haber–Bosch process, which produces NH_3 through the catalytic synthesis of H_2 and N_2 over an iron-based catalyst, is not long-term viable because it requires high temperatures (400–500 °C) and high pressures (150–250 bar), using enormous amounts of fossil fuels and generating a lot of CO_2.[105] Nitrogen photofixation is the reaction of nitrogen gas (or nitrate) in the presence of water, catalyzed by a semiconductor and light. It generally occurs at

Table 7 The challenges associated with CO_2 reduction to HCOOH and possible solutions

Challenges	Solutions
• Low production efficiency	✓ Developing photocatalysts with high surface area, fast separation of charges, long charge lifetime, efficient light absorption, and appropriate band gap
• Controlling the CO_2 reduction pathway for CO and HCOOH is challenging since they are key elements in producing other hydrocarbons	✓ Tuning the reaction conditions and better understanding the single reaction pathways
• Developing an efficient photocatalyst with co-catalyst modifications	✓ CuO has shown a high affinity for CO_2, designing a catalyst able to activate the hydride transfer pathway (H–) instead of proton transfer

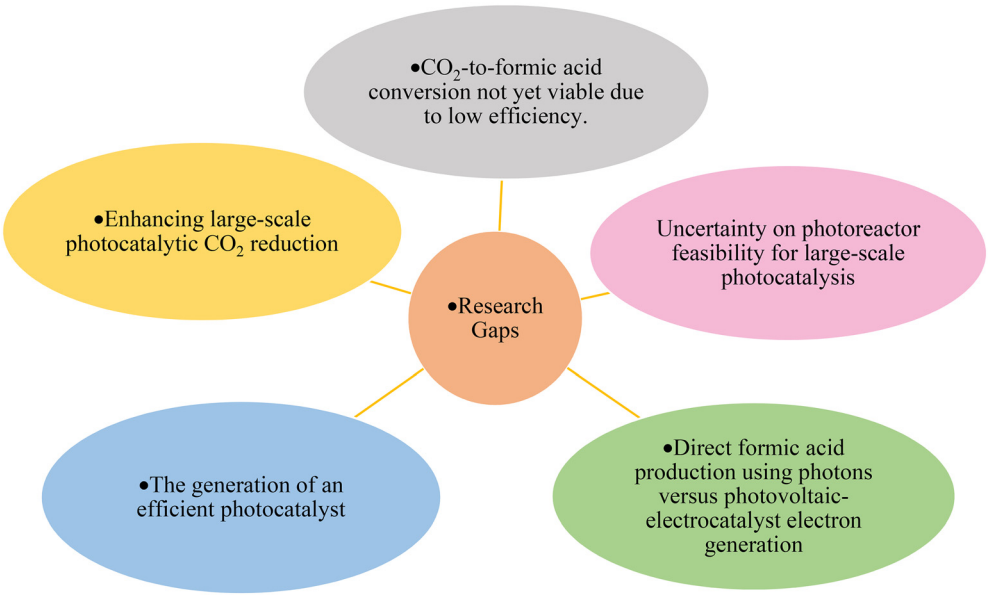

Fig. 13 Research gaps associated with CO_2-to-formic acid conversion.

ambient conditions, reducing the environmental impact associated with the Haber–Bosch process. The general mechanism of nitrogen fixation involves the reaction of water with photo-generated holes (h^+) (eqn (13)), producing oxygen and protons (H^+), followed by the reaction of nitrogen (N_2), protons (H^+) and electrons to produce NH_3 (eqn (14)).[106]

$$3H_2O + 6h^+ + \rightarrow \frac{3}{2}O_2 + 6H^+ \quad (13)$$

$$N_2 + 6H^+ + 6e^- \rightarrow 2NH_3 \quad (14)$$

The overall reaction of ammonia production (eqn (15))

$$N_2 + 3H_2O \rightarrow 2NH_3 + \frac{3}{2}O_2 \quad (15)$$

Tungsten oxides and tungsten trioxide (WO_3) were introduced earlier in 1986 by Endoh *et al.*[107] in a heterogeneous photoreduction of nitrogen to produce ammonia. The reaction occurred by exposing moist N_2 to WO_3 or sub stoichiometric WO_{3-x}, or using sub stoichiometric tungsten oxide dispersions in N_2-saturated aqueous solutions.[107] Later, tungsten trioxide was modified and used in conjunction with other doping materials and different reaction conditions, for example using C/WO_3–H_2O, as reported previously.[108]

An interesting experimental approach was introduced in 2014 by Oshikiri *et al.*,[109] involving the plasmon-induced technique for NH_3 synthesis using visible light irradiation, as shown in Fig. 14, at room temperature. It involved a strontium titanate ($SrTiO_3$) semiconductor photoelectrode loaded with gold (Au) nanoparticles and doped with 0.05 wt.% niobium (Nb–$SrTiO_3$). The photoelectrochemical reaction cell is split into two-section chambers to provide an efficient separation between the oxidized products (on the anodic side) and reduced (on the cathodic side), enhancing the NH_3 formation. The rate of formation of NH_3 is 0.231 nmol h^{-1}.[109]

The use of graphitic carbon nitride (g-C_3N_4) in combination with other composites has generated significant interest in nitrogen photofixation, as demonstrated in various experimental studies over the last decade.[110–114] Notably, the reported yield using g-C_3N_4 composites surpasses that of other photocatalysts, highlighting its promising potential in this field.

N_2 gas is not the only feedstock for the production of ammonia. The reduction of nitrate has also been explored. Tong *et al.*[115] reported on the photocatalytic synthesis of NH_3 by the reduction of nitrate (NO_3^-) under UV irradiation, using a PdSn/NiO/$NaTaO_3$:La photocatalyst in the presence of HCOOH in an aqueous solution. Nitrate is used because it is one of the most widespread water contaminants. It is hazardous to both human health and the ecosystem. Several factors were evaluated, including the initial concentration and pH of nitrate, plus the co-catalyst loading. The photocatalyst was doped with 5% bimetallic PdSn and 0.2% NiO loadings. This was done to achieve a high efficiency of NH_3 production due to the efficient electron–hole pair separation of PdSn acting as an electron trap and the strong affinity of NiO to adsorb nitrite.

Moreover, aqueous HCOOH was adopted as a hole scavenger due to its strong reducing property, the ability to supply carboxyl anion radicals for nitrate reduction, and *in situ* buffer effect on NH_3 reduction. This resulted in a remarkable nitrogen conversion, reaching 100% and NH_3 selectivity of 72% within 2 hours. The experiment was carried out in an immersion well reactor connected to a

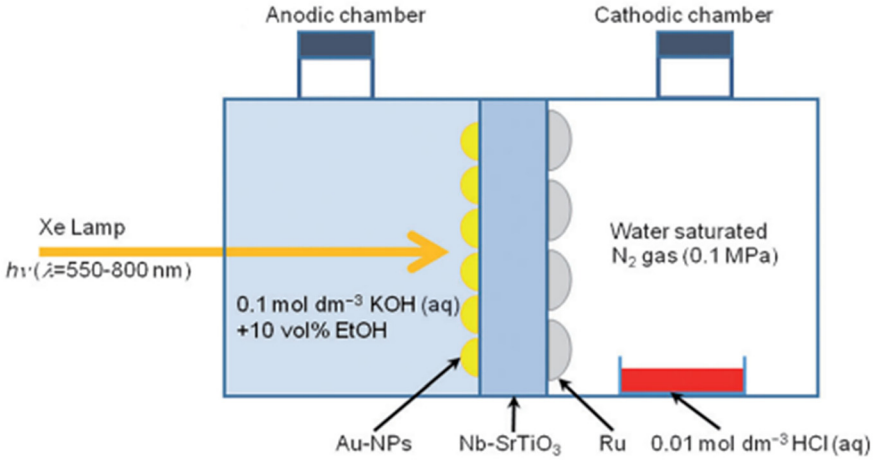

Fig. 14 Schematic of a plasmon-induced device for the photoelectrochemical synthesis of ammonia. Reproduced with permission from ref. 109. Copyright John Wiley & Sons.

closed gas circulation system, including a high-pressure mercury lamp as the light source. The temperature remained constant at 5 °C.[115]

Other studies have emphasized the crucial significance of oxygen vacancies in enhancing the photocatalytic reaction, as reported by ref. 116 and 117. G. Zhang *et al.*[117] specifically investigated the role of oxygen vacancies in TiO_2. One can observe a substantial difference in the yield between TiO_2 and oxygen vacancies compared to another study by Walls *et al.* using a Pd–TiO_2 photocatalyst.[118]

Photocatalytic nitrogen fixation was investigated using Bi/$InVO_4$ by Dong *et al.*[119] They found that 5% Bi/$InVO_4$ reached the optimal photocatalytic performance with a rate that was 5.3 times higher compared to pure $InVO_4$. The increased activity reported can be attributed to the surface plasmon resonance (SPR) induced by metallic Bi, which enhances light absorption and facilitates the efficient separation of charge carriers.[119]

In 2022, C. Li *et al.*[120] investigated a novel perspective on enhancing the performance of photocatalytic nitrogen fixation by employing catalysts that possess oxygen vacancies. N-doping TiO_2 hollow microspheres with oxygen vacancies were introduced. The structure improved the efficiency and stability of nitrogen photofixation.[120]

Several factors can affect the performance of photocatalysts in a reaction. There has been an attempt to improve photocatalysis through heterojunction catalysts such as zinc oxide/zinc sulfide (ZnO@ZnS), which was conducted by Guo *et al.*[121] The composite catalysts can address the issues of low carrier separation efficiency and inadequate light absorption capacity commonly found in individual catalysts.[121,122]

Another factor is the synthesis pathways, which are also quite important. In a study conducted by Huo *et al.*,[123] they used a facile solvothermal route and applied the heat treatment method for BMO@BOC heterojunctions photocatalyst synthesis, demonstrating improved photocatalytic efficiency.[123]

Other studies were conducted on tailoring specific catalysts with preferable activity in photocatalysis reactions. For example, a novel approach was devised to boost the photocatalytic efficiency by testing bismuth oxyhalides having the lowest thermodynamic energy barrier for photocatalytic nitric oxide oxidation reaction.[124]

A recent study was performed by Morawski *et al.*[125] that involved the green synthesis of NH_3 from gaseous nitrogen and CO_2-saturated water vapor. A novel gas phase photocatalytic reactor, including a bed in the form of UV transparent glass fiber cloth coated with titanium dioxide (P25 TiO_2), was used (Fig. 15). The bed is located just above the water surface. The gases circulate from the top to the water surface, where NH_3 gas is produced and directly gets dissolved in the water phase, continuously separating the ammonia from the gas phase and immediately shifting the equilibrium to the product side. The highest ammonia production was 1.3 mmol NH_4^+ g_{cat} after 6 hours at 20 °C. The presence of CO_2 caused a gas phase reduction to carbon monoxide (100 μmol CO/g TiO_2/dm^3), CH_4 (7 μmol CH_4/g TiO_2/dm^3), and H_2 (1–2 μmol H_2/g TiO_2/dm^3). A rise in temperature from 20 °C to 50 °C did not remarkably increase

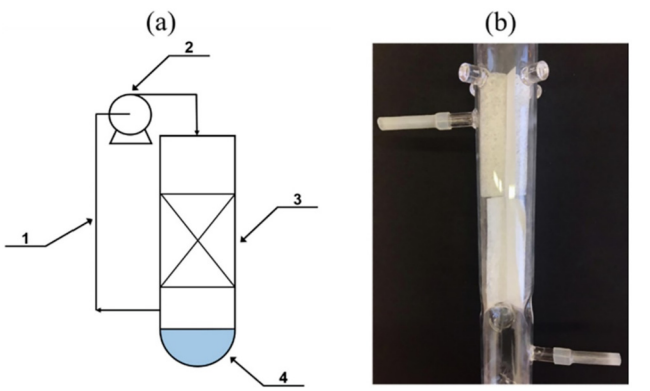

Fig. 15 The reactor diagram: (a) 1 – circulation loop; 2 – pump; 3 – photocatalyst on a glass fiber cloth; 4 – water; (b) the quartz reactor bed. Reproduced with permission from ref. 125 under the terms of the CC BY license.

Table 8 The performance of the catalysts for nitrogen photofixation

Catalyst	Temperature	Light irradiation	N_2 source	NH_3 yield	Ref.
$C/WO_3{\cdot}H_2O$	25 °C	UV-vis	N_2	205 μmol g^{-1} h^{-1}	108
g-C_3N_4/rGO	30 °C	Visible	Air	515 μM g^{-1} h^{-1}	110
g-C_3N_4/MgAlFeO	30 °C	Visible	N_2	417 μM g^{-1} h^{-1}	111
PdSn/NiO/$NaTaO_3$:La	5 °C	UV	NO_3^-	3.6 mmol	115
MXene-derived TiO_2@C/g-C_3N_4	—	Visible	N_2	250.6 μmol g^{-1} h^{-1}	113
SiW_{12}/K-C_3N_4	25 °C	UV	N_2	353.2 μM g^{-1} h^{-1}	112
Pd–TiO_2	25 °C	UV	N_2	21.2 mmol	118
TiO_2 (oxygen vacancies)	25 °C	UV-vis	N_2	324.86 μmol g^{-1} h^{-1}	117
(OV–$In(OH)_3$/CN)	25 °C	Visible	N_2	3.81 mM h^{-1} g^{-1}	116
Bi/$InVO_4$	25 °C	—	N_2	626 μmol g^{-1} h^{-1}	119
g-C_3N_4/MgZnAl-MMO	25 °C	Visible	N_2	47.56 μmol L^{-1}	114
AN/BiOBr–Cl	—	Visible	N_2	234.4 μmol g^{-1} h^{-1}	127
La/MoO_3-*x*	25 °C	Visible	N_2	209.0 μmol g^{-1} h^{-1}	128
Fe–WO_3	55 °C	UV-vis	Air	477 μg g^{-1} h^{-1}	126
N–TiO_2 (oxygen vacancies)	—	Visible	N_2	80.09 μmol g^{-1} h^{-1}	120

the yield of ammonia. However, it did eliminate the production of CO. No CH_4 was produced when the NH_3 yield increased, regardless of the temperature. The ammonium ions that are dissolved in water were in the form of ammonium hydrogen carbonate NH_4HCO_3 or ammonium carbonate $(NH_4)_2CO_3$. Whereas in the case of pure nitrogen, it appears as NH_4OH.[125]

Another experiment was conducted by Shen *et al.*[126] of a photocatalytic nitrogen fixation using air and visible light as the light source under mild conditions. The photocatalyst used is tungsten trioxide (WO_3) doped with iron (Fe) prepared by high-temperature calcination. The Fe-doped WO_3 contains oxygen vacancies that are introduced to fix the nitrogen from the air at atmospheric pressure. The highest nitrogen fixation rate (nitrogen reduction) can increase to 477 μg g_{cat}^{-1}.[126] Table 8 compiles a comprehensive range of catalysts investigated and reported in nitrogen photofixation.

2.3.1 Challenges and potential solutions. Table 9 presents the challenges associated with ammonia synthesis and associated solutions, which can overcome the bottlenecks of this process.

2.3.2 Research gaps. The following research gaps are identified based on the previous literature work, as presented in Fig. 16.[129,130]

In the field of nitrogen photofixation, introducing an electrical field (hence, photo-electrocatalysis) could represent a winning strategy for enhancing the efficiency of NH_3 production. In fact, including an electrical source in the photoconversion process is a significant topic of discussion, as it is essential to determine whether it would result in a higher yield of NH_3 and improved process efficiency. Additionally, it is imperative to investigate how the introduction of electricity would impact the catalyst and its stability. In general, as discussed for the other processes, it is necessary to develop efficient catalysts with high stability and activity to perform the NH_3 reaction and increase the selectivity towards ammonia, reducing the probability of other undesired by-products. One of the major issues with nitrogen photofixation is the quick oxidation of the NH_3 product to nitrate due to the simulataneous redox reaction. Numerous methods have been proposed to address this issue, including removing the product during the reaction, separating the catalyst suspension from the reaction, and utilizing plasmon-induced techniques to isolate the two reaction chambers. Nevertheless, the efficacy of these approaches in resolving this challenge has not been fully validated. Further investigation is required to explore the feasibility of carrying out the reaction in a gaseous state due to the inherent lack of solubility of nitrogen gas in aqueous solutions, which has been identified as a limiting factor in achieving a satisfactory level of NH_3 conversion.

Table 9 Challenges associated with the photocatalytic synthesis of ammonia and possible solutions

Challenges	Solutions
• Poor activity, poor selectivity towards NH_3, and low reaction yields	✓ NiO has demonstrated strong adsorption of nitrite, using electron donors to consume the photogenerated holes (*e.g.*, formic acid), using oxides characterized by high oxygen vacancies
• Quick oxidation of ammonia to nitrate	✓ Quickly separating the reaction products if they are produced in the same chamber, separating the catalyst from water suspension or performing the photofixation in the gas phase
• Above 50 °C, the ammonia yield decreases	✓ The temperature of the reaction should be controlled; the ammonia reaction is reversible and shifts towards the products at low temperature

Source: compiled from ref. 129 and 130.

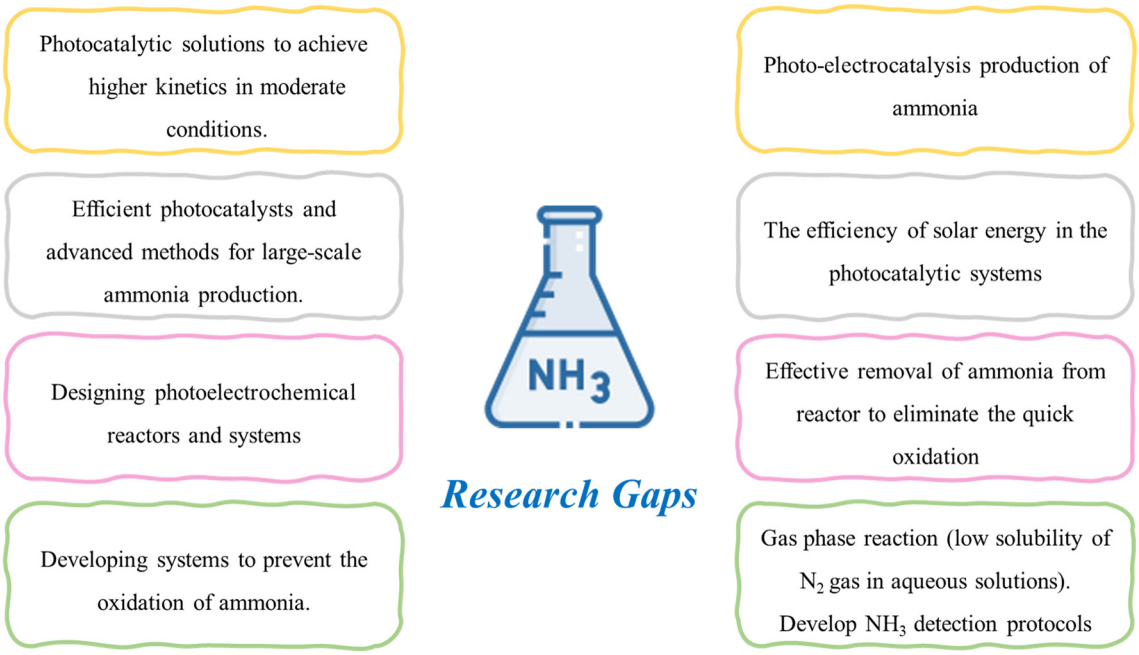

Fig. 16 Areas requiring further investigation for successful nitrogen fixation.

Despite the existence of multiple studies demonstrating the feasibility of photocatalytic nitrogen fixation technology at the laboratory level, there is a lack of research examining its practicality and viability when implemented on a larger scale. Hence, there is a pressing need for further research to bridge this gap and facilitate the commercialization of this promising technology.

3. Comparative evaluation

This section presents a concise assessment of the three green fuels, HCOOH, CH_3OH, and NH_3 based on the reviewed literature. The four processes discussed in this review have been compared in terms of production yield and photoproduction selectivity *versus* the conventional methods' selectivity. In this comparison, the selectivity benchmark technologies used are the conversion of CO_2 into HCOOH through catalytic hydrogenation of CO_2, and the production of NH_3 *via* steam reforming of methane/Haber–Bosch process and CH_3OH *via* the steam reforming of methane/catalytic hydrogenation of CO_2, as illustrated in Table 10.

Table 10 provides an overview of the catalysts that have exhibited outstanding performance, and display promising potential for the four technologies. Among the four technologies, POM exhibits the highest selectivity with a value of 98.7%, followed by HCOOH with a range between 80–90%. Photocatalytic nitrogen fixation technology reported the lowest selectivity (72%). This is attributed to the reversible nature of the reaction, which can be affected by a change in reaction conditions such as temperature and pressure.

When the photocatalytic processes of CH_3OH, HCOOH, and NH_3 are compared with the benchmark technologies currently being used, a promising trend was observed that could displace the conventional processes in the future. The selectivity data obtained for HCOOH and CH_3OH production, through CO_2 reduction and partial oxidation of CH_4, demonstrates a strong correlation with benchmark technologies. This alignment is highly advantageous in the context of photocatalytic CO_2 reduction, as it significantly reduces energy consumption compared to conventional processes. Moreover, using renewable energy sources, coupled with reaction conditions at ambient temperatures and pressures, overcomes the requirement for additional downstream separation steps to enhance selectivity. The selectivity of Haber–Bosch technology has very low selectivity

Table 10 The highest reported yield and selectivity for the four technologies

Criteria	Formic acid	Ammonia	Methanol (CO_2 reduction)	Methanol (POM)
Yield ($\mu mol\ g^{-1}\ h^{-1}$)	3500 (ref. 103)	626 (ref. 119)	2910 (ref. 3)	4500 (ref. 83)
Selectivity (%)	80–90 (ref. 100)	72 (ref. 115)	98 (ref. 131)	98.7 (ref. 73)
Benchmark technology selectivity (%)	96[a]	20–25[a]	95–98[a]	95–98[a]

[a] Benchmark technology selectivity compiled from ref. 132–136.

(20–25%) compared to nitrogen photofixation (72%) due to the equilibrium and kinetic limitations of the reaction, resulting in by-product formation.

The main purpose of photocatalysis is to utilize abundant and easily accessible sunlight as an energy source to initiate and drive reactions, thereby eliminating the need for additional energy inputs. This has significant implications for reducing reliance on fossil fuels and minimizing the environmental footprint associated with traditional energy-intensive processes. The value reported of the energy consumption of the steam reforming of methane/catalytic hydrogenation of CO_2 technology ranges between 28–32 GJ per ton of CH_3OH produced.[135,136]

It is important to highlight that photocatalytic technologies are still at an early stage of development, particularly in the context of NH_3 production, and several challenges need to be addressed. Besides the yield of the reaction, the key focal points that should be tackled are the fast oxidation of NH_3 to nitrate, low stability of N_2 in water, and poor activity. Further research is required to investigate the solution of separating the redox products during the reaction to avoid NH_3 oxidation and the importance of conducting photoreduction of NH_3 in the gas phase.

Notably, the literature and experimental data on NH_3 and HCOOH production were found to be relatively limited. On the other hand, there has been a notable increase in exploration and research activity regarding the partial oxidation of CH_4 and CO_2 reduction to CH_3OH over the past five years, both holding promising potential for industrial implementation within the next decade.

For photocatalytic CH_3OH production, an additional oxygen source should be introduced to enhance the POM reaction, such as oxygen and hydrogen peroxide (H_2O_2). Additionally, a pressurized stainless steel batch reactor for POM can significantly improve the reaction outcomes, with pressures ranging from 2 to 3 MPa.

The reduction of CO_2 to CH_3OH and HCOOH poses significant challenges in controlling the CO_2 reduction pathway, as it inhibits further reaction and produces other undesired hydrocarbons. Furthermore, there is a need to develop a scalable system to make these processes economically viable in terms of reactor design and reaction conditions.

4. Conclusions

This review highlights the importance of the photocatalytic process in producing green fuels. Herein, we discussed the photoproduction of three different types of fuels, including the fundamentals, significance, concepts, and mechanism. In addition, the fuel synthesis methods, different catalysts used, experimental setups, reaction conditions, and reactor design were specifically identified, addressed, and evaluated. Upon thorough evaluation, this review has identified and presented the main challenges and potential solutions associated with four photocatalytic technologies. Furthermore, research directions to address the existing research gaps, paving the way for further advancements in the field of photocatalysis of CH_4, CO_2 and NH_3 have been highlighted.

Through the research conducted, synthesis method, and results obtained in order to enhance the photocatalytic activity, the following points were concluded:

- Guarantee effective separation of the electron–hole pair of the photocatalyst by providing doping or co-catalysts (such as carbon-based supports).
- Employing an appropriate bandgap energy for the photocatalyst to ensure photon absorption *via* effective light sources.
- Developing photocatalysts with high surface area, fast separation of charges, long charge lifetime, efficient light absorption, and appropriate band gap.
- Enhancing the reaction kinetics by adding sacrificial agents to utilize photo-generated electrons.
- Tuning the reaction conditions, such as operating temperature and light irradiation, to improve the effectiveness of single reaction pathways.

Further research should be done to understand and clarify ways in which secondary NH_3 oxidation could be prevented. For CH_4 conversion through partial oxidation, doping the catalysts with metals, metal oxides, and non-metals or using metal–organic framework (MOFs) catalysts are suggested. The development of photoreactors that allow the reaction to be carried out effectively on a large scale is subjected to ongoing development.

Author contributions

Amira Chebbi: conceptualization, methodology, formal analysis, writing – original draft. Alessandro Sinopoli: conceptualization, writing – review & editing. Ahmed Abotaleb: writing – review & editing. Yusuf Bicer: conceptualization, methodology, writing – review & editing, supervision.

Conflicts of interest

There are no conflicts to declare.

Acknowledgements

The authors acknowledge the support provided by Hamad Bin Khalifa University, Qatar Foundation, Qatar (210051864).

References

1 J. Hansen, M. Sato, G. Russell and P. Kharecha, Climate sensitivity, sea level and atmospheric carbon dioxide, *Philos. Trans. R. Soc., A*, 2013, **371**(2001), 20120294.
2 P. E. Thornton, S. C. Doney, K. Lindsay, J. K. Moore, N. Mahowald and J. T. Randerson, Carbon-nitrogen interactions regulate climate-carbon cycle feedbacks: results from an atmosphere-ocean general circulation model, *Biogeosciences*, 2009, **6**(10), 2099–2120.

3 Y. N. Kavil, Y. A. Shaban, M. I. Orif, R. Al-Farawati and S. U. M. K. Mousa Zobidi, Production of Methanol as a Fuel Energy from CO2 What Is So Different About Present in Polluted Seawater - A Photocatalytic Neuroenhancement? Was ist so anders am Neuroenhancement? Outlook, *Open Chem.*, 2018, **16**, 1089–1098.
4 United States Environmental Protection Agency, *Greenhouse Gas Inventory Data Explorer|US EPA*, Greenhouse Gas Inventory Data Explorer - All Sectors, 2020.
5 J. Ran, M. Jaroniec and S. Z. Qiao, Cocatalysts in Semiconductor-based Photocatalytic CO2 Reduction: Achievements, Challenges, and Opportunities, *Adv. Mater.*, 2018, **30**(7), 1704649.
6 R. B. Jackson, M. Saunois, P. Bousquet, J. G. Canadell, B. Poulter and A. R. Stavert, *et al.*, Increasing anthropogenic methane emissions arise equally from agricultural and fossil fuel sources, *Environ. Res. Lett.*, 2020, **15**(7), 071002.
7 M. Saunois, A. Stavert, B. Poulter, P. Bousquet, J. Canadell and R. B. Jackson, *et al.*, The global methane budget 2000-2017, *Earth Syst. Sci. Data*, 2020, **12**(3), 1561–1623.
8 S. Kirschke, P. Bousquet, P. Ciais, M. Saunois, J. G. Canadell and E. J. Dlugokencky, *et al.*, Three decades of global methane sources and sinks, *Nat. Geosci.*, 2013, **6**(10), 813–823.
9 M. Saunois, R. B. Jackson, P. Bousquet, B. Poulter and J. G. Canadell, The growing role of methane in anthropogenic climate change, *Environ. Res. Lett.*, 2016, **11**(12), 120207.
10 J. Lang, Y. Ma, X. Wu, Y. Jiang and Y. H. Hu, Highly efficient light-driven methane coupling under ambient conditions based on an integrated design of a photocatalytic system, *Green Chem.*, 2020, **22**(14), 4669–4675.
11 P. Machado, A. Amaral, S. Carminati, R. Januário, S. Ferreira and P. Moreira Vaz, *et al.*, Photocatalytic Methane Conversion over Pd/ZnO Photocatalysts under Mild Conditions, *Methane*, 2023, **2**(1), 44–55.
12 Methane Tracker 2020 – Analysis – IEA, 2020.
13 Overview – Global Methane Tracker 2022 – Analysis – IEA, 2022.
14 A. Banu and Y. Bicer, Review on COx-free hydrogen from methane cracking: Catalysts, solar energy integration and applications, *Energy Convers. Manage.: X*, 2021, **12**, 100117.
15 U. P. M. Ashik, W. M. A. Wan Daud and H. F. Abbas, Production of greenhouse gas free hydrogen by thermocatalytic decomposition of methane – A review, *Renewable Sustainable Energy Rev.*, 2015, **44**, 221–256.
16 H. F. Abbas and W. M. A. Wan Daud, Hydrogen production by methane decomposition: A review, *Int. J. Hydrogen Energy*, 2010, **35**(3), 1160–1190.
17 T. Karchiyappan, A Review On Hydrogen Energy Production From Electrochemical System: Benefits And Challenges, *Energy Sources, Part A*, 2018, **41**(7), 902–909, DOI: **10.1080/15567036.2018.1520368**.
18 H. M. Torres Galvis, J. H. Bitter, T. Davidian, M. Ruitenbeek, A. I. Dugulan and K. P. De Jong, Iron particle size effects for direct production of lower olefins from synthesis gas, *J. Am. Chem. Soc.*, 2012, **134**(39), 16207–16215.
19 R. M. Navarro, M. A. Peña and J. L. G. Fierro, Hydrogen production reactions from carbon feedstocks: Fossil fuels and biomass, *Chem. Rev.*, 2007, **107**(10), 3952–3991.
20 G. A. Olah, A. Goeppert, M. Czaun and G. K. S. Prakash, Bi-reforming of Methane from Any Source with Steam and Carbon Dioxide Exclusively to Metgas (CO–2H2) for Methanol and Hydrocarbon Synthesis, *J. Am. Chem. Soc.*, 2012, **135**(2), 648–650.
21 L. Mo, K. K. M. Leong and S. Kawi, A highly dispersed and anti-coking Ni–La2O3/SiO2 catalyst for syngas production from dry carbon dioxide reforming of methane, *Catal. Sci. Technol.*, 2014, **4**(7), 2107–2114.
22 J. M. Lavoie, Review on dry reforming of methane, a potentially more environmentally-friendly approach to the increasing natural gas exploitation, *Front. Chem.*, 2014, **2**(NOV), 81.
23 M. S. Fan, A. Z. Abdullah and S. Bhatia, Catalytic Technology for Carbon Dioxide Reforming of Methane to Synthesis Gas, *ChemCatChem*, 2009, **1**(2), 192–208.
24 X. Wu, L. Xu, M. Chen, C. Lv, X. Wen and Y. Cui, *et al.*, Recent Progresses in the Design and Fabrication of Highly Efficient Ni-Based Catalysts With Advanced Catalytic Activity and Enhanced Anti-coke Performance Toward CO2 Reforming of Methane, *Front. Chem.*, 2020, **8**, 850.
25 A. G. S. Hussien and K. Polychronopoulou, A Review on the Different Aspects and Challenges of the Dry Reforming of Methane (DRM) Reaction, *Nanomaterials*, 2022, **12**(19), 3400.
26 L. Weger, A. Abánades and T. Butler, Methane cracking as a bridge technology to the hydrogen economy, *Int. J. Hydrogen Energy*, 2017, **42**(1), 720–731.
27 N. Sánchez-Bastardo, R. Schlögl and H. Ruland, Methane Pyrolysis for Zero-Emission Hydrogen Production: A Potential Bridge Technology from Fossil Fuels to a Renewable and Sustainable Hydrogen Economy, *Ind. Eng. Chem. Res.*, 2021, **60**(32), 11855–11881.
28 J. G. Canadell, C. Le Quéré, M. R. Raupach, C. B. Field, E. T. Buitenhuis and P. Ciais, *et al.*, Contributions to accelerating atmospheric CO2 growth from economic activity, carbon intensity, and efficiency of natural sinks, *Proc. Natl. Acad. Sci. U. S. A.*, 2007, **104**(47), 18866–18870.
29 K. L. Denman, G. Brasseur, A. Chidthaisong, P. Ciais, P. Cox and R. E. Dickinson, *et al.*, Couplings Between Changes in the Climate System and Biogeochemistry Coordinating Lead Authors: This chapter should be cited as, in *Climate Change 2007: The Physical Science Basis Contribution of Working Group I to the Fourth Assessment Report of the Intergovernmental Panel on Climate Change*, 2007, pp. 499–587.
30 J. Rockström, O. Gaffney, J. Rogelj, M. Meinshausen, N. Nakicenovic and H. J. Schellnhuber, A roadmap for rapid decarbonization, *Science*, 2017, **355**(6331), 1269–1271.
31 A. Goeppert, M. Czaun, G. K. Surya Prakash and G. A. Olah, Air as the renewable carbon source of the future: an

overview of CO2 capture from the atmosphere, *Energy Environ. Sci.*, 2012, **5**(7), 7833–7853.
32 Y. Abdullatif, A. Sodiq, N. Mir, Y. Bicer, T. Al-Ansari and M. H. El-Naas, *et al.*, Emerging trends in direct air capture of CO2: a review of technology options targeting net-zero emissions, *RSC Adv.*, 2023, **13**(9), 5687–5722.
33 K. S. Lackner, Carbonate Chemistry for Sequestering Fossil Carbon, *Annu. Rev. Energy Environ.*, 2002, **27**, 193–232.
34 A. Saravanan, P. Senthil Kumar, D. V. N. Vo, S. Jeevanantham, V. Bhuvaneswari and V. Anantha Narayanan, *et al.*, A comprehensive review on different approaches for CO2 utilization and conversion pathways, *Chem. Eng. Sci.*, 2021, **236**, 116515.
35 C. G. Okoye-Chine, K. Otun, N. Shiba, C. Rashama, S. N. Ugwu and H. Onyeaka, *et al.*, Conversion of carbon dioxide into fuels—A review, *J. CO2 Util.*, 2022, **62**, 102099.
36 V. Fetisov, A. M. Gonopolsky, M. Y. Zemenkova, S. Andrey, H. Davardoost and A. H. Mohammadi, *et al.*, On the Integration of CO2 Capture Technologies for an Oil Refinery, *Energies*, 2023, **16**(2), 865.
37 M. Aziz, A. TriWijayanta and A. B. D. Nandiyanto, Ammonia as Effective Hydrogen Storage: A Review on Production, Storage and Utilization, *Energies*, 2020, **13**(12), 3062.
38 C. Zamfirescu and I. Dincer, Ammonia as a green fuel and hydrogen source for vehicular applications, *Fuel Process. Technol.*, 2009, **90**(5), 729–737.
39 H. Kobayashi, A. Hayakawa, K. D. K. A. Somarathne and E. C. Okafor, Science and technology of ammonia combustion, *Proc. Combust. Inst.*, 2019, **37**(1), 109–133.
40 I. Rafiqul, C. Weber, B. Lehmann and A. Voss, Energy efficiency improvements in ammonia production—perspectives and uncertainties, *Energy*, 2005, **30**(13), 2487–2504, Available from: **https://www.sciencedirect.com/science/article/pii/S0360544204004943**.
41 H. Shen, C. Choi, J. Masa, X. Li, J. Qiu and Y. Jung, *et al.*, Electrochemical ammonia synthesis: Mechanistic understanding and catalyst design, *Chem*, 2021, **7**(7), 1708–1754.
42 M. E. Gálvez, A. Frei, M. Halmann and A. Steinfeld, Ammonia Production *via* a Two-Step Al2O3/AlN Thermochemical Cycle. 2. Kinetic Analysis, *Ind. Eng. Chem. Res.*, 2007, **46**(7), 2047–2053.
43 P. Mohanty, K. K. Pant, S. N. Naik, J. Parikh, A. Hornung and J. N. Sahu, Synthesis of green fuels from biogenic waste through thermochemical route – The role of heterogeneous catalyst: A review, *Renewable Sustainable Energy Rev.*, 2014, **38**, 131–153.
44 J. He, Z. Li, X. Zhang, H. Wang, W. Dong and E. Du, *et al.*, Towards carbon neutrality: A study on China's long-term low-carbon transition pathways and strategies, *Environ. Sci. Ecotechnology*, 2022, **9**, 100134.
45 S. C. Sherwood, V. Dixit and C. Salomez, The global warming potential of near-surface emitted water vapour, *Environ. Res. Lett.*, 2018, **13**(10), 104006.
46 EPA, Understanding Global Warming Potentials|US EPA, *Greenh Gas Emiss.*, 2022, pp. 1–5.
47 L. Spadaro, F. Arena and A. Palella, Which Future Route in the Methanol Synthesis? Photocatalytic Reduction of CO2, the New Challenge in the Solar Energy Exploitation, *Methanol: Science and Engineering*, Elsevier B.V., 2018, pp. 429–472.
48 G. Yuniar, W. H. Saputera, D. Sasongko, R. R. Mukti, J. Rizkiana and H. Devianto, Recent Advances in Photocatalytic Oxidation of Methane to Methanol, *Molecules*, 2022, **27**(17), 5496.
49 J. Wang, C. Hao, Q. Zhang, Q. Meng and H. Liu, Research advances on photo-assisted CO2 conversion to methanol, *Appl. Catal., A*, 2022, **643**(June), 118738.
50 W. Zhang, Y. Hu, L. Ma, G. Zhu, Y. Wang and X. Xue, *et al.*, Progress and Perspective of Electrocatalytic CO2 Reduction for Renewable Carbonaceous Fuels and Chemicals, *Adv. Sci.*, 2018, **5**(1), 1700275.
51 X. Li, L. Wang, W. Su and Y. Xing, A review of the research status of CO2 photocatalytic conversion technology based on bibliometrics, *New J. Chem.*, 2021, **45**(5), 2315–2325.
52 L. Liu and Y. Li, Understanding the Reaction Mechanism of Photocatalytic Reduction of CO2 with H2O on TiO2-Based Photocatalysts: A Review, *Aerosol Air Qual. Res.*, 2014, **14**(2), 453–469.
53 F. Solymosi and I. Tombácz, Photocatalytic reaction of H2O +CO2 over pure and doped Rh/TiO2, *Catal. Lett.*, 1994, **27**(1–2), 61–65.
54 Q. D. Truong, J. Y. Liu, C. C. Chung and Y. C. Ling, Photocatalytic reduction of CO 2 on FeTiO 3/TiO 2 photocatalyst, *Catal. Commun.*, 2012, **19**, 85–89.
55 S. P. Cheng, L. W. Wei and H. P. Wang, Photocatalytic Reduction of CO2 to Methanol by Cu2O/TiO2 Heterojunctions, *Sustainability*, 2022, **14**(1), 374.
56 V. D. B. C. Dasireddy and B. Likozar, Photocatalytic CO2 reduction to methanol over bismuth promoted BaTiO3 perovskite nanoparticle catalysts, *Renewable Energy*, 2022, **195**, 885–895.
57 Y. Liu, Y. Yang, Q. Sun, Z. Wang, B. Huang and Y. Dai, *et al.*, Chemical adsorption enhanced CO2 capture and photoreduction over a copper porphyrin based metal organic framework, *ACS Appl. Mater. Interfaces*, 2013, **5**(15), 7654–7658.
58 W. Dai, X. Hu, T. Wang, W. Xiong, X. Luo and J. Zou, Hierarchical CeO 2 /Bi 2 MoO 6 heterostructured nanocomposites for photoreduction of CO 2 into hydrocarbons under visible light irradiation, *Appl. Surf. Sci.*, 2018, **434**, 481–491.
59 L. Wang, M. Ghoussoub, H. Wang, Y. Shao, W. Sun and A. A. Tountas, *et al.*, Photocatalytic Hydrogenation of Carbon Dioxide with High Selectivity to Methanol at Atmospheric Pressure, *Joule*, 2018, **2**, 1369–1381.
60 S. Pocoví-Martínez, I. Zumeta-Dube and D. Diaz, Production of methanol from aqueous CO2 by using Co3O4 nanostructures as photocatalysts, *J. Nanomater.*, 2019, **2019**, 6461493, DOI: **10.1155/2019/6461493**.
61 O. Shtyka, R. Ciesielski, A. Kedziora, W. Maniukiewicz, S. Dubkov and D. Gromov, *et al.*, Photocatalytic Reduction of

CO2 Over Me (Pt, Pd, Ni, Cu)/TiO2 Catalysts, *Top. Catal.*, 2020, **63**(1–2), 113–120.
62 S. Kazemi Movahed, A. Najinasab, R. Nikbakht and M. Dabiri, Visible light assisted photocatalytic reduction of CO2 to methanol using Fe3O4@N-C/Cu2O nanostructure photocatalyst, *J. Photochem. Photobiol., A*, 2020, **401**, 112763.
63 J. Albo and G. García, Enhanced visible-light photoreduction of CO2 to methanol over Mo2C/TiO2 surfaces in an optofluidic microreactor, *React. Chem. Eng.*, 2021, **6**(2), 304–312.
64 H. Xi, Y. Xu, W. Zou, J. Ji, Y. Cai and H. Wan, *et al.*, Enhanced methanol selectivity of CuxO/TiO2 photocatalytic CO2 reduction: Synergistic mechanism of surface hydroxyl and low-valence copper species, *J. CO2 Util.*, 2022, **55**, 101825.
65 C. Candia-Onfray, S. Rojas, M. V. B. Zanoni and R. Salazar, An updated review of metal–organic framework materials in photo(electro)catalytic applications: From CO2 reduction to wastewater treatments, *Curr. Opin. Electrochem.*, 2021, **26**, 100669.
66 K. Sonowal, N. Nandal, P. Basyach, L. Kalita, S. L. Jain and L. Saikia, Photocatalytic reduction of CO2 to methanol using Zr(IV)-based MOF composite with g-C3N4 quantum dots under visible light irradiation, *J. CO2 Util.*, 2022, **57**, 101905.
67 N. Li, X. Liu, J. Zhou, W. Chen and M. Liu, Encapsulating CuO quantum dots in MIL-125(Ti) coupled with g-C3N4 for efficient photocatalytic CO2 reduction, *Chem. Eng. J.*, 2020, **399**, 125782.
68 H. Yu, Y. Xuan, Q. Zhu and S. Chang, Highly efficient and stable photocatalytic CO2 and H2O reduction into methanol at lower temperatures through an elaborate gas–liquid–solid interfacial system, *Green Chem.*, 2023, **25**(2), 596–605.
69 W. Yu, D. Xu and T. Peng, Enhanced photocatalytic activity of g-C3N4 for selective CO2 reduction to CH3OH *via* facile coupling of ZnO: a direct Z-scheme mechanism, *J. Mater. Chem. A*, 2015, **3**(39), 19936–19947.
70 L. Wang, M. Ghoussoub, H. Wang, Y. Shao, W. Sun and A. A. Tountas, *et al.*, Photocatalytic Hydrogenation of Carbon Dioxide with High Selectivity to Methanol at Atmospheric Pressure, *Joule*, 2018, **2**(7), 1369–1381.
71 K. Ogura and M. Kataoka, Photochemical conversion of methane, *J. Mol. Catal.*, 1988, **43**(3), 371–379.
72 J. Xie, R. Jin, A. Li, Y. Bi, Q. Ruan and Y. Deng, *et al.*, Highly selective oxidation of methane to methanol at ambient conditions by titanium dioxide-supported iron species, *Nat. Catal.*, 2018, **1**(11), 889–896.
73 Z. Zhang, J. Zhang, Y. Zhu, Z. An, X. Shu and H. Song, *et al.*, Photo-splitting of water toward hydrogen production and active oxygen species for methane activation to methanol on Co-SrTiO3, *Chem Catal.*, 2022, **2**(6), 1440–1449.
74 J. Yang, J. Hao, J. Wei, J. Dai and Y. Li, Visible-light-driven selective oxidation of methane to methanol on amorphous FeOOH coupled m-WO3, *Fuel*, 2020, **266**, 117104.
75 K. Villa, S. Murcia-López, T. Andreu and J. R. Morante, On the role of WO3 surface hydroxyl groups for the photocatalytic partial oxidation of methane to methanol, *Catal. Commun.*, 2015, **58**, 200–203.
76 K. Villa, S. Murcia-López, T. Andreu and J. R. Morante, Mesoporous WO3 photocatalyst for the partial oxidation of methane to methanol using electron scavengers, *Appl. Catal., B*, 2015, **163**, 150–155.
77 H. Song and J. Ye, Direct photocatalytic conversion of methane to value-added chemicals, *Trends Chem.*, 2022, 1094–1105.
78 Z. Ma, Y. Chen, C. Gao and Y. Xiong, A Minireview on the Role of Cocatalysts in Semiconductor-Based Photocatalytic CH4Conversion, *Energy Fuels*, 2022, **36**(19), 11428–11442.
79 Y. Hu, Y. Nagai, D. Rahmawaty, C. Wei and M. Anpo, Characteristics of the photocatalytic oxidation of methane into methanol on V-containing MCM-41 catalysts, *Catal. Lett.*, 2008, **124**(1–2), 80–84.
80 S. Murcia-López, K. Villa, T. Andreu and J. R. Morante, Partial oxidation of methane to methanol using bismuth-based photocatalysts, *ACS Catal.*, 2014, **4**(9), 3013–3019.
81 J. A. de Oliveira, J. C. da Cruz, O. R. Nascimento and C. Ribeiro, Selective CH4 reform to methanol through partial oxidation over Bi2O3 at room temperature and pressure, *Appl. Catal., B*, 2022, **318**, 121827.
82 Y. Yi, Z. Tang, X. Wu, A. Huang, X. Luo and G. Q. Xu, *et al.*, Photocatalytic oxidation of methane to methanol by tungsten trioxide-supported atomic gold at room temperature, *Appl. Catal., B*, 2022, **306**, 120919.
83 X. Zhang, Y. Wang, K. Chang, S. Yang, H. Liu and Q. Chen, *et al.*, Constructing hollow porous Pd/H-TiO2 photocatalyst for highly selective photocatalytic oxidation of methane to methanol with O2, *Appl. Catal., B*, 2023, **320**, 121961.
84 Y. Negishi, S. Watanabe, M. Aoki, S. Hossain, W. Kurashige and Y. Negishi, *et al.*, Toward the Creation of Highly Active Photocatalysts That Convert Methane into Methanol, *Concepts Semicond. Photocatal.*, 2019, 85–97.
85 J. Wang, R. Li, D. Zeng, W. Wang, Y. Zhang and L. Zhang, *et al.*, Photocatalytic conversion of methane selectively into oxygenated products in the presence of chloride ions, *Chem. Eng. J.*, 2023, **452**, 139505.
86 H. Du, X. Li, Z. Cao, S. Zhang, W. Yu and F. Sun, *et al.*, Photocatalytic O2 oxidation of CH4 to CH3OH on AuFe-ZnO bifunctional catalyst, *Appl. Catal., B*, 2023, **324**, 122291.
87 N. Dhabarde, J. Selvaraj, A. Yuda, A. Kumar and V. R. Subramanian, Review of photocatalytic and photo-electrocatalytic reduction of CO2 on carbon supported films, *Int. J. Hydrogen Energy*, 2022, **47**(72), 30908–30936.
88 T. Rasheed, S. Shafi, M. T. Anwar, K. Rizwan, T. Ahmad and M. Bilal, Revisiting photo and electro-catalytic modalities for sustainable conversion of CO2, *Appl. Catal., A*, 2021, **623**, 118248.
89 D. A. Bulushev and J. R. H. Ross, Towards Sustainable Production of Formic Acid, *ChemSusChem*, 2018, **11**(5), 821–836.
90 B. Thijs, J. Rongé and J. A. Martens, Matching emerging formic acid synthesis processes with application requirements, *Green Chem.*, 2022, **24**(6), 2287–2295.

91 F. Pan, B. Li, W. Deng, Z. Du, Y. Gang and G. Wang, *et al.*, Promoting electrocatalytic CO2 reduction on nitrogen-doped carbon with sulfur addition, *Appl. Catal., B*, 2019, **252**, 240–249.
92 H. Shen, T. Peppel, J. Strunk and Z. Sun, Photocatalytic Reduction of CO2 by Metal-Free-Based Materials: Recent Advances and Future Perspective, *Sol. RRL*, 2020, **4**(8), 1900546.
93 S. M. Aliwi and K. F. Al-Jubori, Photoreduction of CO2 by metal sulphide semiconductors in presence of H2S, *Sol. Energy Mater.*, 1989, **18**(3–4), 223–229.
94 K. Maeda, K. Sekizawa and O. Ishitani, A polymeric-semiconductor–metal-complex hybrid photocatalyst for visible-light CO2 reduction, *Chem. Commun.*, 2013, **49**(86), 10127–10129.
95 A. Nakada, K. Koike, T. Nakashima, T. Morimoto and O. Ishitani, Photocatalytic CO2 reduction to formic acid using a Ru(II)-Re(I) supramolecular complex in an aqueous solution, *Inorg. Chem.*, 2015, **54**(4), 1800–1807.
96 O. Omadoko, D. Scott, R. Hickman and D. L. Myers, Simple photoreduction of carbon dioxide to formic acid and true quantum yield, *Phys. Chem. Chem. Phys.*, 2020, **22**(8), 4632–4639.
97 H. Zhang, Y. Li, J. Wang, N. Wu, H. Sheng and C. Chen, *et al.*, An unprecedent hydride transfer pathway for selective photocatalytic reduction of CO2 to formic acid on TiO2, *Appl. Catal., B*, 2021, **284**, 119692.
98 K. Mori, J. Matsuo, Y. Kondo, H. Hata and H. Yamashita, Photoreduction of Carbon Dioxide to Formic Acid with Fe-Based MOFs: The Promotional Effects of Heteroatom Doping and Alloy Nanoparticle Confinement, *ACS Appl. Energy Mater.*, 2021, **4**(10), 11634–11642.
99 L. I. Ibarra-Rodriguez, J. C. Pantoja-Espinoza, E. Luévano-Hipólito, L. F. Garay-Rodríguez, A. López-Ortiz and L. M. Torres-Martínez, *et al.*, Formic acid and hydrogen generation from the photocatalytic reduction of CO2 on visible light activated N-TiO2/CeO2/CuO composites, *J. Photochem. Photobiol.*, 2022, **11**, 100125.
100 D. An, S. Nishioka, S. Yasuda, T. Kanazawa, Y. Kamakura and T. Yokoi, *et al.*, Alumina-Supported Alpha-Iron(III) Oxyhydroxide as a Recyclable Solid Catalyst for CO2 Photoreduction under Visible Light, *Angew. Chem., Int. Ed.*, 2022, **61**(26), e202204948.
101 L. Wang, L. Wang, S. Yuan, L. Song, H. Ren and Y. Xu, *et al.*, Covalently-bonded single-site Ru-N2 knitted into covalent triazine frameworks for boosting photocatalytic CO2 reduction, *Appl. Catal., B*, 2023, **322**, 122097.
102 G. Mele, C. Annese, A. De Riccardis, C. Fusco, L. Palmisano and G. Vasapollo, *et al.*, Turning lipophilic phthalocyanines/TiO2 composites into efficient photocatalysts for the conversion of CO2 into formic acid under UV–vis light irradiation, *Appl. Catal., A*, 2014, **481**, 169–172.
103 D. O. Adekoya, M. Tahir and N. A. S. Amin, g-C 3 N 4 /(Cu/TiO 2) nanocomposite for enhanced photoreduction of CO 2 to CH 3 OH and HCOOH under UV/visible light, *J. CO2 Util.*, 2017, **18**, 261–274.
104 N. Gruber and J. N. Galloway, An Earth-system perspective of the global nitrogen cycle, *Nature*, 2008, **451**(7176), 293–296.
105 J. M. McEnaney, A. R. Singh, J. A. Schwalbe, J. Kibsgaard, J. C. Lin and M. Cargnello, *et al.*, Ammonia synthesis from N2 and H2O using a lithium cycling electrification strategy at atmospheric pressure, *Energy Environ. Sci.*, 2017, **10**(7), 1621–1630.
106 M. Nazemi and M. A. El-Sayed, Plasmon-enhanced photo(electro)chemical nitrogen fixation under ambient conditions using visible light responsive hybrid hollow Au-Ag2O nanocages, *Nano Energy*, 2019, **63**, 103886.
107 E. Endoh, J. K. Leland and A. J. Bard, Heterogeneous photoreduction of nitrogen to ammonia on tungsten oxide, *J. Phys. Chem.*, 1986, **90**(23), 6223–6226, DOI: **10.1021/j100281a031**.
108 X. Li, W. Wang, D. Jiang, S. Sun, L. Zhang and X. Sun, Efficient Solar-Driven Nitrogen Fixation over Carbon–Tungstic-Acid Hybrids, *Chem. – Eur. J.*, 2016, **22**(39), 13819–13822.
109 T. Oshikiri, K. Ueno and H. Misawa, Plasmon-Induced Ammonia Synthesis through Nitrogen Photofixation with Visible Light Irradiation, *Angew. Chem., Int. Ed.*, 2014, **53**(37), 9802–9805, DOI: **10.1002/anie.201404748**.
110 S. Hu, W. Zhang, J. Bai, G. Lu, L. Zhang and G. Wu, Construction of a 2D/2D g-C3N4/rGO hybrid heterojunction catalyst with outstanding charge separation ability and nitrogen photofixation performance *via* a surface protonation process, *RSC Adv.*, 2016, **6**(31), 25695–25702.
111 Y. Wang, W. Wei, M. Li, S. Hu, J. Zhang and R. Feng, *In situ* construction of Z-scheme g-C3N4/Mg1.1Al0.3Fe0.2O1.7 nanorod heterostructures with high N2 photofixation ability under visible light, *RSC Adv.*, 2017, **7**(29), 18099–18107.
112 C. Xiao, L. Zhang, K. Wang, H. Wang, Y. Zhou and W. Wang, A new approach to enhance photocatalytic nitrogen fixation performance *via* phosphate-bridge: a case study of SiW12/K-C3N4, *Appl. Catal., B*, 2018, **239**, 260–267.
113 Q. Liu, L. Ai and J. Jiang, MXene-derived TiO2@C/g-C3N4 heterojunctions for highly efficient nitrogen photofixation, *J. Mater. Chem. A*, 2018, **6**(9), 4102–4110.
114 J. S. Prabagar, D. Vinod, Y. Sneha, K. M. Anilkumar, S. Rtimi and K. Wantala, *et al.*, Novel gC3N4/MgZnAl-MMO derived from LDH for solar-based photocatalytic ammonia production using atmospheric nitrogen, *Environ. Sci. Pollut. Res.*, 2022, 1–14.
115 N. Tong, Y. Wang, Y. Liu, M. Li, Z. Zhang and H. Huang, *et al.*, PdSn/NiO/NaTaO3:La for photocatalytic ammonia synthesis by reduction of NO3− with formic acid in aqueous solution, *J. Catal.*, 2018, **361**, 303–312.
116 J. Fan, M. Zuo, Z. Ding, Z. Zhao, J. Liu and B. Sun, A readily synthesis of oxygen vacancy-induced In(OH)3/carbon nitride 0D/2D heterojunction for enhanced visible-light-driven nitrogen fixation, *Chem. Eng. J.*, 2020, **396**, 125263.
117 G. Zhang, X. Yang, C. He, P. Zhang and H. Mi, Constructing a tunable defect structure in TiO2 for photocatalytic nitrogen fixation, *J. Mater. Chem. A*, 2019, **8**(1), 334–341.

118 J. M. Walls, J. S. Sagu and K. G. Upul Wijayantha, Microwave synthesised Pd-TiO 2 for photocatalytic ammonia production, *RSC Adv.*, 2019, **9**(11), 6387–6394.
119 J. Wang, C. Hua, X. Dong, Y. Wang and N. Zheng, Synthesis of plasmonic bismuth metal deposited InVO4 nanosheets for enhancing solar light-driven photocatalytic nitrogen fixation, *Sustainable Energy Fuels*, 2020, **4**(4), 1855–1862.
120 C. Li, M. Z. Gu, M. M. Gao, K. N. Liu, X. Y. Zhao and N. W. Cao, *et al.*, N-doping TiO2 hollow microspheres with abundant oxygen vacancies for highly photocatalytic nitrogen fixation, *J. Colloid Interface Sci.*, 2022, **609**, 341–352.
121 Z. Guo, W. Huo, T. Cao, X. Liu, S. Ren and J. Yang, *et al.*, Heterojunction interface of zinc oxide and zinc sulfide promoting reactive molecules activation and carrier separation toward efficient photocatalysis, *J. Colloid Interface Sci.*, 2021, **588**, 826–837.
122 T. Cao, W. Huo, Z. Guo, C. Jing, Y. Chen and Y. Zhang, *et al.*, Constructing defective (BiO)2CO3 with different dominated facets for efficiently photocatalytic NO oxidization and *in situ* reaction pathway study, *Appl. Surf. Sci.*, 2019, **498**, 143848.
123 W. Huo, T. Cao, W. Xu, Z. Guo, X. Liu and H. C. Yao, *et al.*, Facile construction of Bi2Mo3O12@Bi2O2CO3 heterojunctions for enhanced photocatalytic efficiency toward NO removal and study of the conversion process, *Chin. J. Catal.*, 2020, **41**(2), 268–275.
124 W. Huo, W. Xu, Z. Guo, Y. Zhang and F. Dong, Motivated surface reaction thermodynamics on the bismuth oxyhalides with lattice strain for enhanced photocatalytic NO oxidation, *Appl. Catal., B*, 2021, **284**, 119694.
125 A. W. Morawski, K. Ćmielewska, E. Ekiert, E. Kusiak-Nejman, I. Pełech and P. Staciwa, *et al.*, Effective green ammonia synthesis from gaseous nitrogen and CO2 saturated-water vapour utilizing a novel photocatalytic reactor, *Chem. Eng. J.*, 2022, **446**, 137030.
126 Y. Shen, J. Shou, L. Chen, W. Han, L. Zhang and Y. Chen, *et al.*, Efficient photocatalytic nitrogen fixation from air under sunlight *via* iron-doped WO3, *Appl. Catal., A*, 2022, **643**, 118739.
127 M. Lan, N. Zheng, X. Dong, Y. Wang, J. Wu and X. Ren, *et al.*, Application of flexible PAN/BiOBr-Cl microfibers as self-supporting and highly active photocatalysts for nitrogen fixation and dye degradation, *Appl. Surf. Sci.*, 2022, **575**, 151743.
128 X. Liu, Y. Luo, C. Ling, Y. Shi, G. Zhan and H. Li, *et al.*, Rare earth La single atoms supported MoO3-x for efficient photocatalytic nitrogen fixation, *Appl. Catal., B*, 2022, **301**, 120766.
129 G. N. Schrauzer, Photoreduction of Nitrogen on TiO2 and TiO2-Containing Minerals, *Green Energy Technol.*, 2011, **33**, 601–623.
130 S. Zhang, Y. Zhao, R. Shi, G. I. N. Waterhouse and T. Zhang, Photocatalytic ammonia synthesis: Recent progress and future, *EnergyChem*, 2019, **1**(2), 100013.
131 M. L. Gothe, F. J. Pérez-Sanz, A. H. Braga, L. R. Borges, T. F. Abreu and R. C. Bazito, *et al.*, Selective CO2 hydrogenation into methanol in a supercritical flow process, *J. CO2 Util.*, 2020, **40**, 101195.
132 Catalytic hydrogenation of CO2 to formic acid using a highly active and selective ruthenium–phosphine catalyst, *Green Chem.*, 2014, **16**(2), 1865–1869.
133 DOE-OIT US, *Energy and Environmental Profile of the US Chemical Industry*, Prepared by Energetics Incorporated, Columbia, Maryland, USA, 2000.
134 Ammonia Synthesis for Fertilizer Production, *Chem. Eng. Prog.*, 2009, **105**(6).
135 O. Levenspiel, *Chemical Reaction Engineering*, 3rd edn, 1999.
136 K. Westerterp, H. V. Knoef, M. Van Swaaij and G. F. Versteeg, The methanol synthesis process, *Chem. Eng. Sci.*, 2000, **55**(7), 1203–1218.